

EEG-17



**HYDROLOGIC ANALYSES OF TWO BRINE ENCOUNTERS
IN THE VICINITY OF THE WASTE ISOLATION
PILOT PLANT (WIPP) SITE**

Peter Spiegler, Ph.D.
Environmental Evaluation Group
Environmental Improvement Division
Health and Environment Department
State New Mexico

December 1982

CONTENTS

| Title | Page |
|---|------|
| FOREWORD | i |
| STAFF AND CONSULTANTS | ii |
| SUMMARY | iii |
| 1. INTRODUCTION | 1 |
| 2. REDUCTION AND ANALYSIS OF ERDA-6 DATA | 1 |
| 2.1 Geologic profile of ERDA-6 | 1 |
| 2.2 Reservoir Testing Activities | 4 |
| 2.3 Pressure-Buildup Data | 4 |
| 2.4 Flow Data | 17 |
| 3. REDUCTION AND ANALYSIS OF WIPP-12 DATA | 21 |
| 3.1 Geologic Profile of WIPP-12 | 21 |
| 3.2 Reservoir Testing Activities | 21 |
| 3.3 Pressure Buildup Data | 28 |
| 3.4 Flow Data | 38 |
| 4. EXPLANATION OF THE BRINE RESERVOIRS NEAR THE WIPP SITE | 41 |
| 4.1 Pore Volume Compressibility of Fractured Reservoirs | 41 |
| 4.2 Estimated Volume of ERDA-6 | 44 |
| 4.3 Estimated Volume of WIPP-12 | 44 |
| 4.4 Cause of Abnormal Pressure and Age of Reservoirs | 46 |
| 4.5 Correlation of Hydrologic and Seismic Data | 53 |
| 5. EFFECT OF WELL TESTING DATA ON DRILLING SCENARIO..... | 53 |
| APPENDIX A. Analytical tools for Characterizing two-porosity Systems..... | 58 |
| NOMENCLATURE | 61 |
| REFERENCES | 63 |

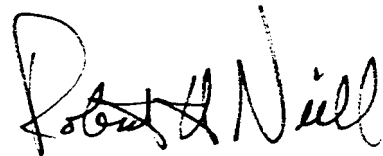
FOREWORD

The purpose of the Environmental Evaluation Group (EEG) is to conduct an independent technical evaluation of the potential radiation exposure to people from the proposed Federal radioactive Waste Isolation Pilot Plant (WIPP) near Carlsbad, in order to protect the public health and safety and ensure that there is minimal environmental degradation. The EEG is part of the Environmental Improvement Division, a component of the New Mexico Health and Environment Department -- the agency charged with the primary responsibility for protecting the health of the citizens of New Mexico.

The Group is neither a proponent nor an opponent of WIPP.

Analyses are conducted of available data concerning the proposed site, the design of the repository, its planned operation, and its long-term stability. These analyses include assessments of reports issued by the U.S. Department of Energy (DOE) and its contractors, other Federal agencies and organizations, as they relate to the potential health, safety and environmental impacts from WIPP.

The project is funded entirely by the U.S. Department of Energy through Contract DE-AC04-79AL10752 with the New Mexico Health and Environment Department.

A handwritten signature in black ink, appearing to read "Robert H. Neill". The signature is written in a cursive style with a large initial "R".

Robert H. Neill
Director

STAFF AND CONSULTANTS

Ann Bancroft, M.A.L., Librarian
James K. Channell, Ph.D., P.E., Environmental Engineer
Lokesh Chaturvedi, Ph.D., Engineering Geologist
Faith, Stuart, B.S., Consulting Geochemist
Luz Elena Garcia, B.B.E., Administrative Secretary
Marshall S. Little⁽¹⁾, M.S., Health Physicist
Jack M. Mobley, B.A., Scientific Liaison Officer
Robert H. Neill, M.S., Director
Jo Anna DeCarlo, Secretary
Peter Spiegler⁽¹⁾ ⁽²⁾, Ph.D. Radiological Health Analyst
Norma I. Silva, Administrative Officer
David Updegraff, M.S., Consulting Hydrologist

⁽¹⁾ Certified, American Board of Health Physics

⁽²⁾ Certified, American College of Radiology

SUMMARY

The data from ERDA-6 indicates a naturally fractured reservoir of the two-porosity type. The best estimate of the volume is about 60 thousand to 120 thousand barrels. The data from WIPP-12 also indicates a naturally fractured reservoir of the two porosity type. The best estimate of the volume is about 5 million to 10 million barrels. The excess pressure above hydrostatic pressure suggests that the reservoirs were formed many millions of years ago. The location of the fractures suggest that their formation may be connected to the tilting of the Delaware Basin as a unit. The effect of the flow testing data on a drilling scenario through the repository many years following its closure is evaluated.

1 INTRODUCTION

This report represents an independent analysis by EEG of the flow and pressure data obtained in the testing of ERDA-6 and WIPP-12, two drillholes which encountered pressurized brine in the vicinity of the WIPP project. The data were obtained from six volumes released by D'Appolonia and known as the "Data File Report ERDA-6 and WIPP-12 testing" (ref. 1). This report is organized in four sections as follows:

1. Reduction and analysis of ERDA-6 data.
2. Reduction and analysis of WIPP-12 data.
3. Explanation of the brine reservoirs near the WIPP site.
4. Effect of well testing data on intrusion scenario.

The first two sections are adequately described by their title. The third section combines the results of the first two sections with work from the scientific literature to estimate the age and size of the reservoirs and to elucidate their mechanism of formation. The fourth section discusses the significance of these data on a long-term radiological consequence study.

2 REDUCTION AND ANALYSIS OF ERDA-6 DATA

2.1 Geologic profile of ERDA-6

The dimensions and the geologic profile of the ERDA-6 borehole are presented in Figure 1. The location of the main fracture where the brine was encountered is based on coring and well logging data. Figure 2 shows the densilog and the compensated neutron log. These logs were obtained prior to the reservoir testing activities.

The densilog shows three fractures from 2710 to 2720 feet while the compensated neutron log indicates a single peaked curve with a maximum porosity of 12%. The fractures are located near the bottom of a 180 feet thick anhydrite layer. The density of the anhydrite fluctuates between 2.90 and 2.95 gm/cc indicating a density slightly less than 2.98 gm/cc, the maximum density of solid anhydrite.

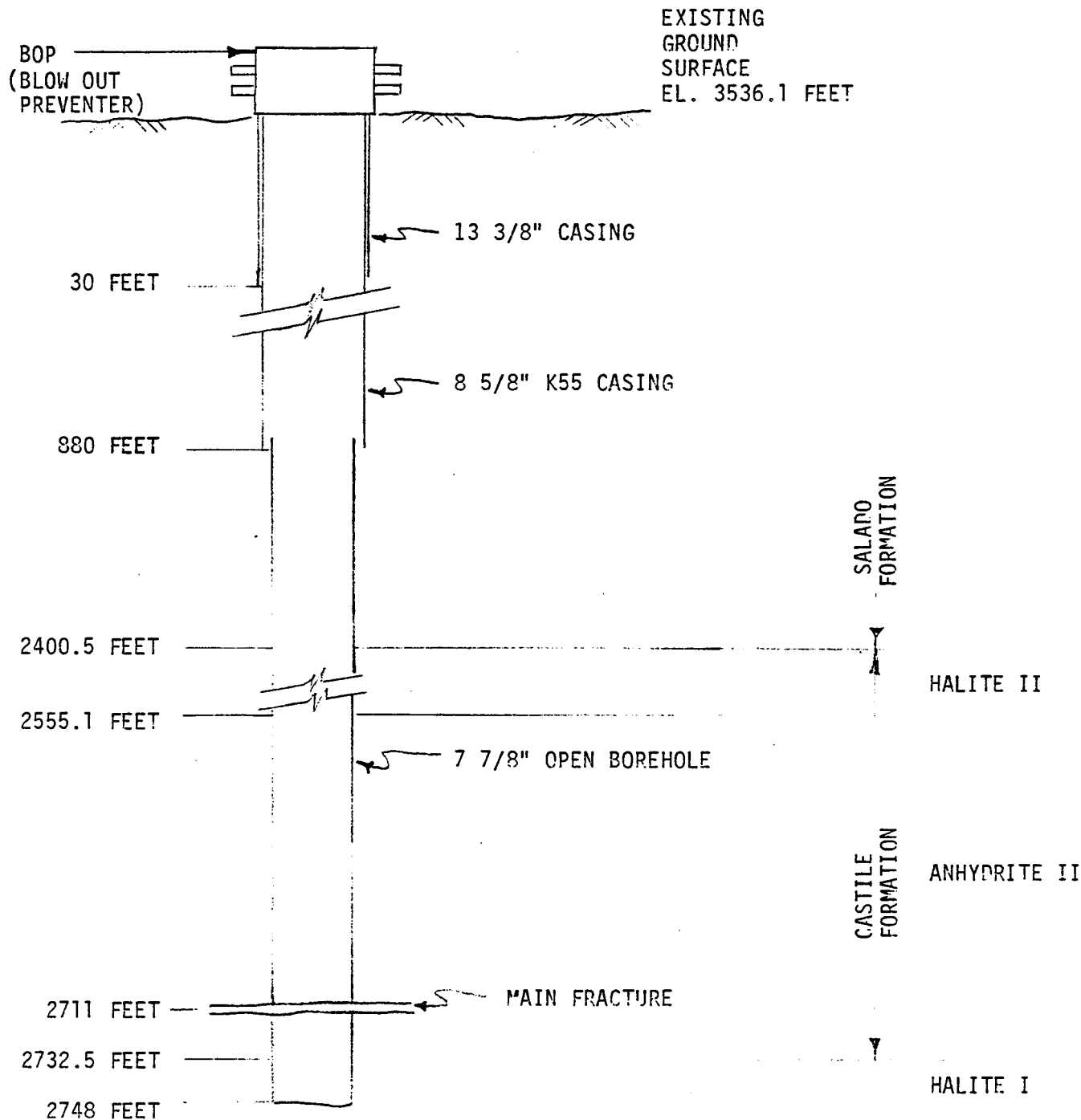


FIGURE NOT TO SCALE

1. DEPTH OF DOWNHOLE COMPONENTS WITH REFERENCE TO GROUND SURFACE.
2. GEOLOGIC PROFILE FROM U.S. GEOLOGICAL SURVEY OPEN-FILE REPORT 81-468.

Figure 1. Geological profile and borehole configuration for ERDA-6
 Figure taken from Reference 1.

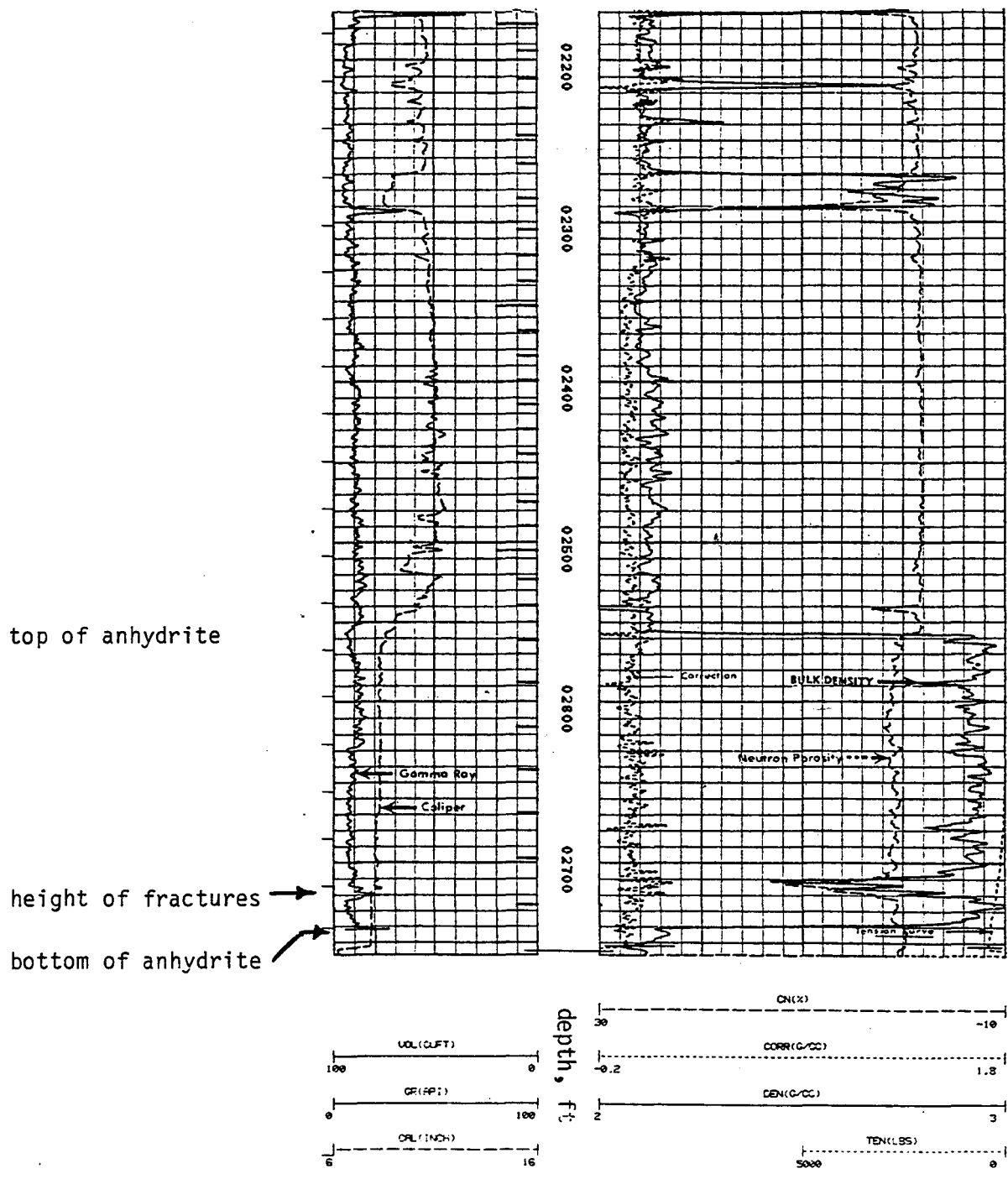


Figure 2. Densilog and compensated neutron log for ERDA-6.
Figure taken from reference 1.

2.2 Reservoir Testing Activities

Two techniques were employed to acquire hydrologic data: drillstem testing (DST), and flow testing with associated subsequent pressure buildup testing.

The arrangement for the DST, is shown in Figure 3. The Lynes packer assembly contained three pressure transducers and three thermocouples. Two of the three pressure transducers, located 47 and 48 feet above the main fracture, measured the pressure in the tested interval. The third transducer, located 50 feet above the main fracture, measured the pressure in the well annulus above the packer. Two drillstem tests, each consisting of two flow periods and two pressure buildup periods, were performed on 10/29/81.

Three constant drawdown-variable discharge rate flow tests were conducted following the DSTs. Flow test #1 was performed with the Lynes packer in place. The brine discharged through the 2 7/8" NSO tubing and pressure was monitored downhole. Flow tests #2 and #3 were performed with the Lynes packer removed. In flow test #2, the pressure buildup following the flow period was monitored at the surface while in flow test #3 the pressure buildup was at first monitored downhole and then at the surface.

Figure 4 summarizes the flow activities.

2.3 Pressure Buildup Data

The pressure-buildup data indicates a naturally fractured reservoir of the two-porosity type. This is illustrated in Figures 5 and 6 which show the pressure buildup versus log time following the final flow period of drillstem test 2680-2 and following flow test #2. The terms at the top of Figure 5 are taken from figure E-1 of reference 2 and are indicated for the following qualitative description of the reservoir: the front end effect curve indicates deep fractures, i.e., fractures that extend far out from the borehole; the infinite acting curve is short, less than 10 minutes, indicating a small region, the first porosity; the boundary curve indicates inflow of brine from the main body of the reservoir, the second porosity. In figure 6 the first porosity is indicated around 10 minutes and the second porosity

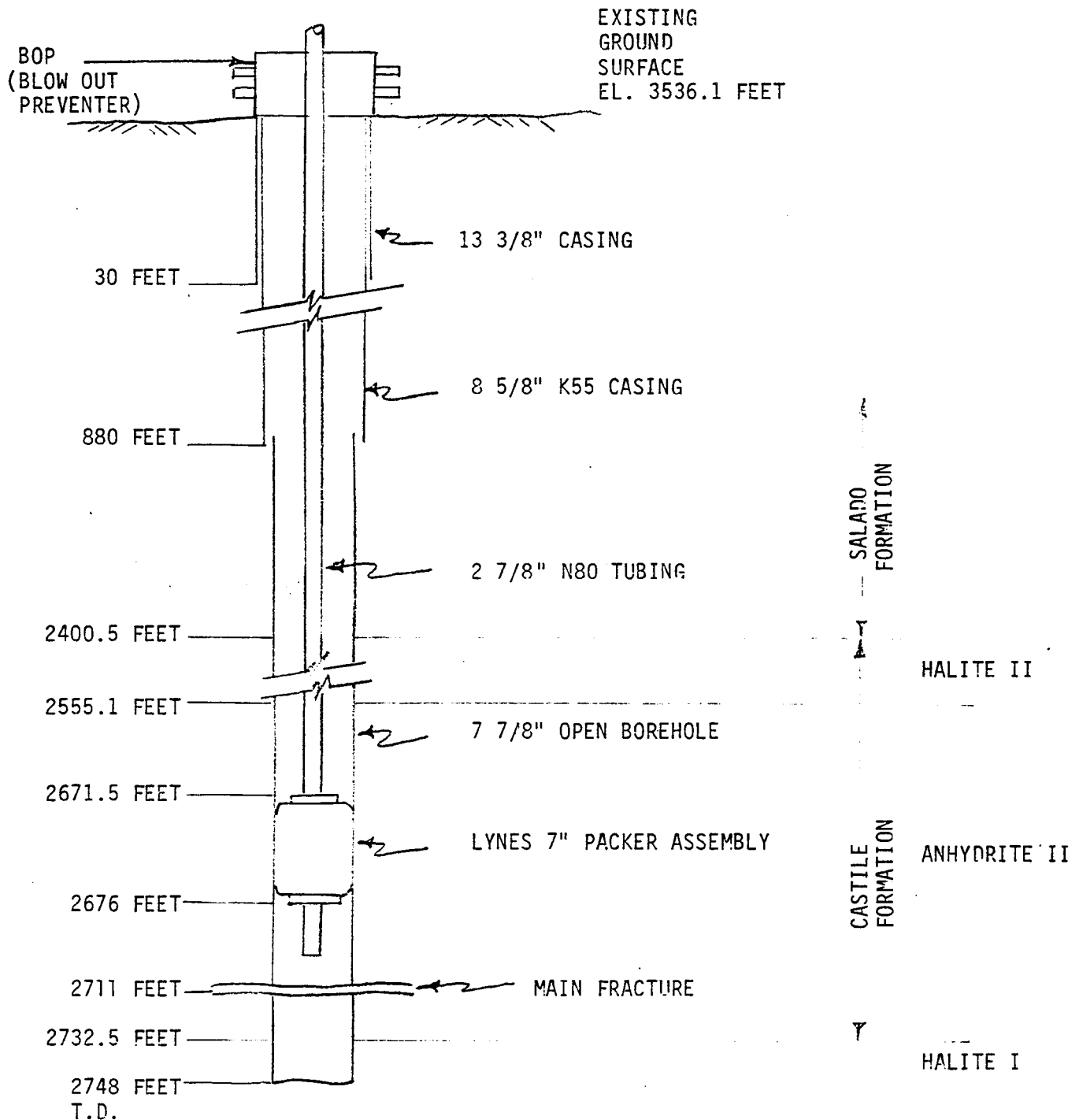
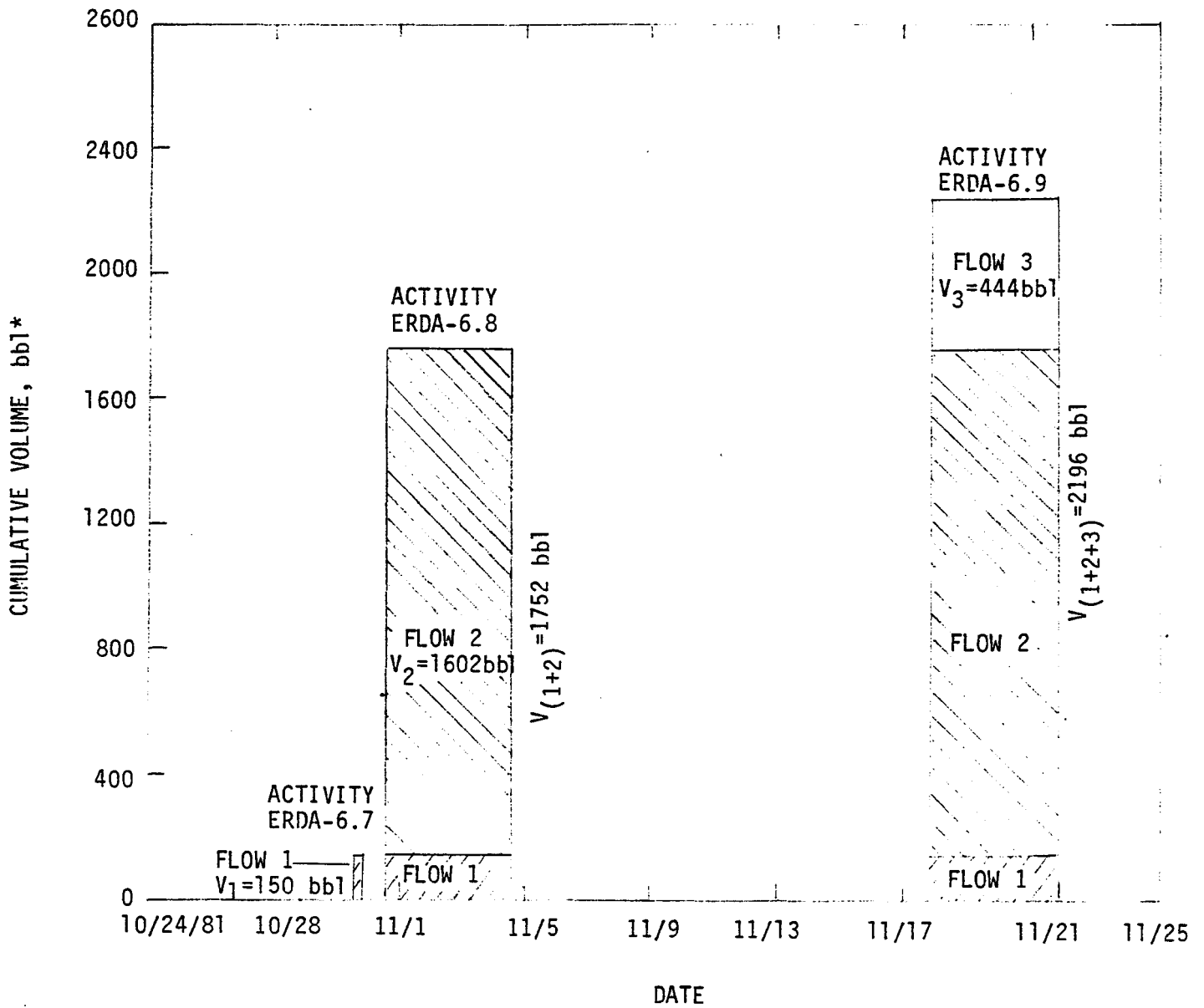


FIGURE NOT TO SCALE

1. DEPTH OF DOWNHOLE COMPONENTS WITH REFERENCE TO GROUND SURFACE.
2. GEOLOGIC PROFILE FROM U.S. GEOLOGICAL SURVEY OPEN FILE REPORT 81-468.

Figure 3. Drillstem test configuration for ERDA-6. Figure taken from Reference 1.



* 1 BARREL (bb1)=42 GALLONS

Figure 4. Summary of flow activities at ERDA-6. Figure taken from Reference 1.

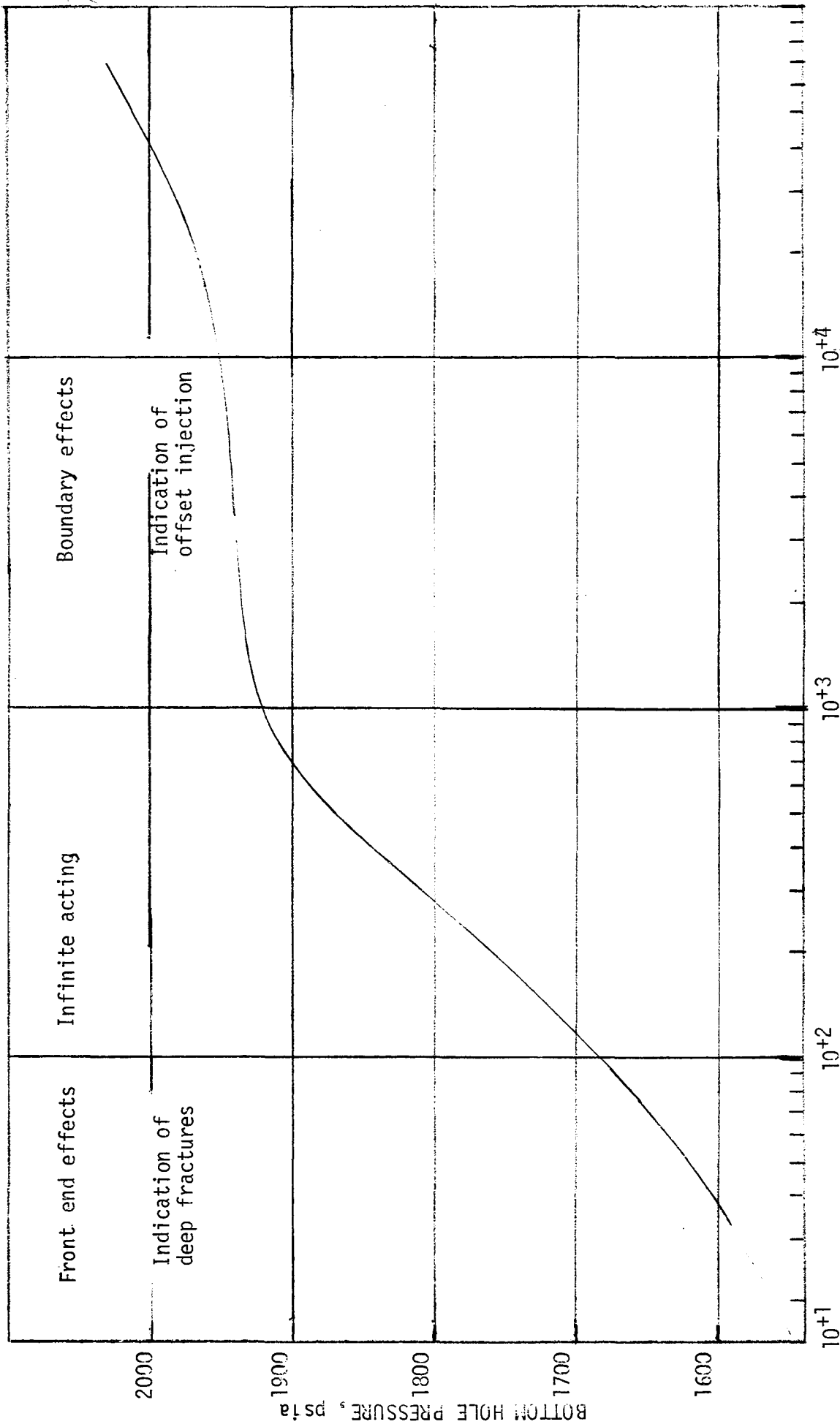


Figure 5. Bottom-hole pressure-buildup for final flow period of drillstem test 2860-2.

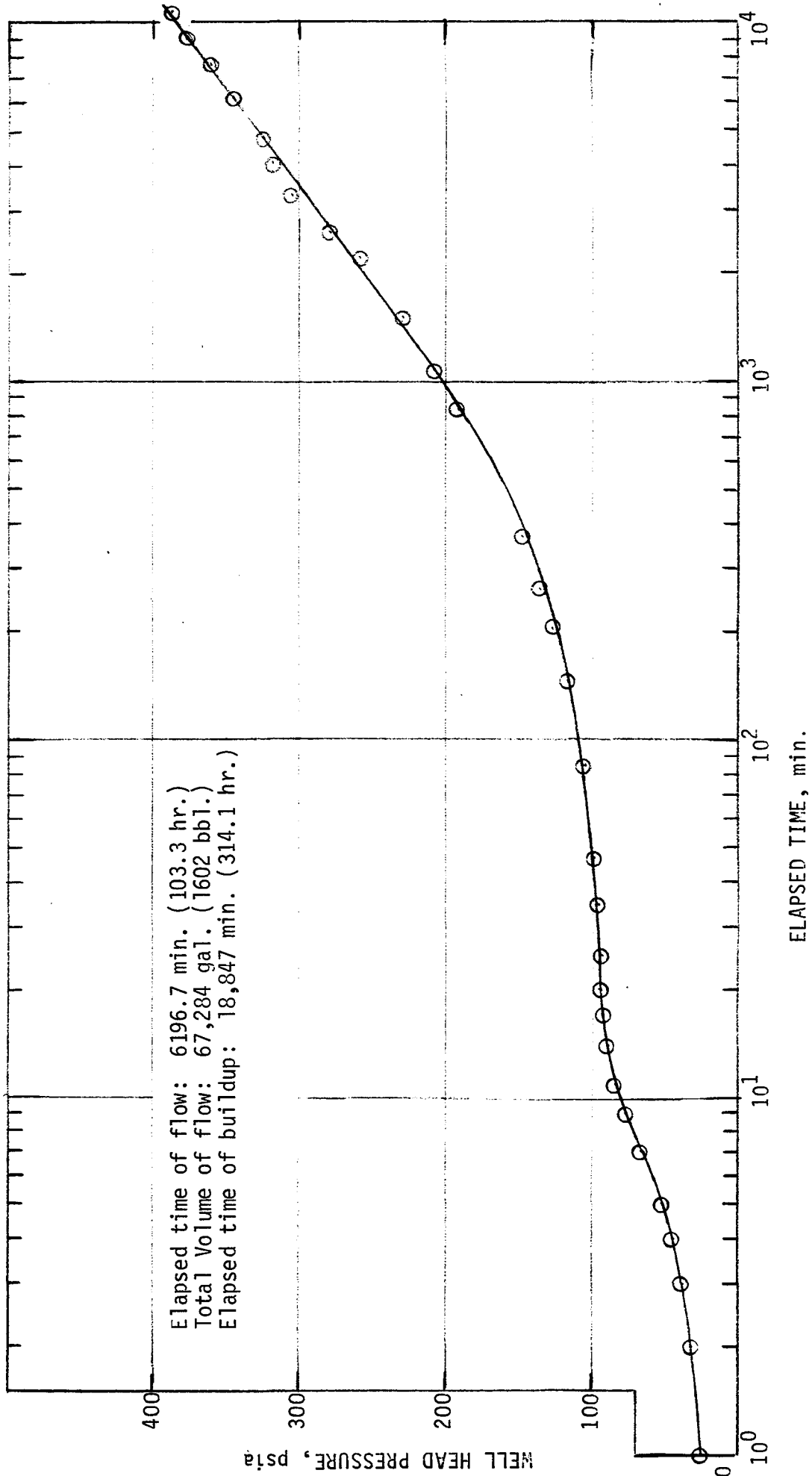


Figure 6. Pressure buildup following flow test #2 at ERDA 6.

after 300 minutes. The DSTs and flow test #1, all with a small outflows of brines, provide data on the first porosity. The pressure buildup following flow tests #2 and #3, both with a larger outflow of brine, provide data on the entire reservoir or both porosities combined.

Figures 7, 8, 9, 10 and 11 are Horner plots of the pressure buildup data while table I is a summary of the permeability calculations using these plots. The following formula is used to calculate the permeability

$$\frac{kh}{\mu} = \frac{162.6q}{m} \quad (1)$$

As already indicated, the DSTs and flow test #1 characterize the region with the first porosity while flow tests #2 and #3 characterize the total of the reservoir. From table I, it is inferred that the ratio of the first permeability to that of the total reservoir is greater than 5 to 1.

Figures 12 shows the Horner plot of the pressure buildup data following flow test #2 and theoretical calculations using parameters in the left-hand corner of the figure and the following formulae (ref. 3)

$$P_{ws}(\Delta t) = p_i - m \log \left[\frac{t+\Delta t}{\Delta t} \right] - \frac{m}{1.151} \left[2\pi t_{pDA} - \frac{1}{2} \ln C_A t_{pDA} \right] - \Delta P_{ws} \quad (2)$$

$$\frac{2.303}{m} \Delta P_{ws} = P_{DMBH}(\Delta t_{DA}) - \ln(t_p + \Delta T) / t_p \quad (3)$$

$$t_{DA} = 0.1835 \frac{qt}{mc_t V_r}$$

Equations (2) and (3) were derived assuming radial fluid flow in a porous medium (see reference 3). However, the mathematics of radial flow is used to extract information from the second straight line of the pressure buildup curve of naturally fractured reservoirs (see reference 2, p.132).

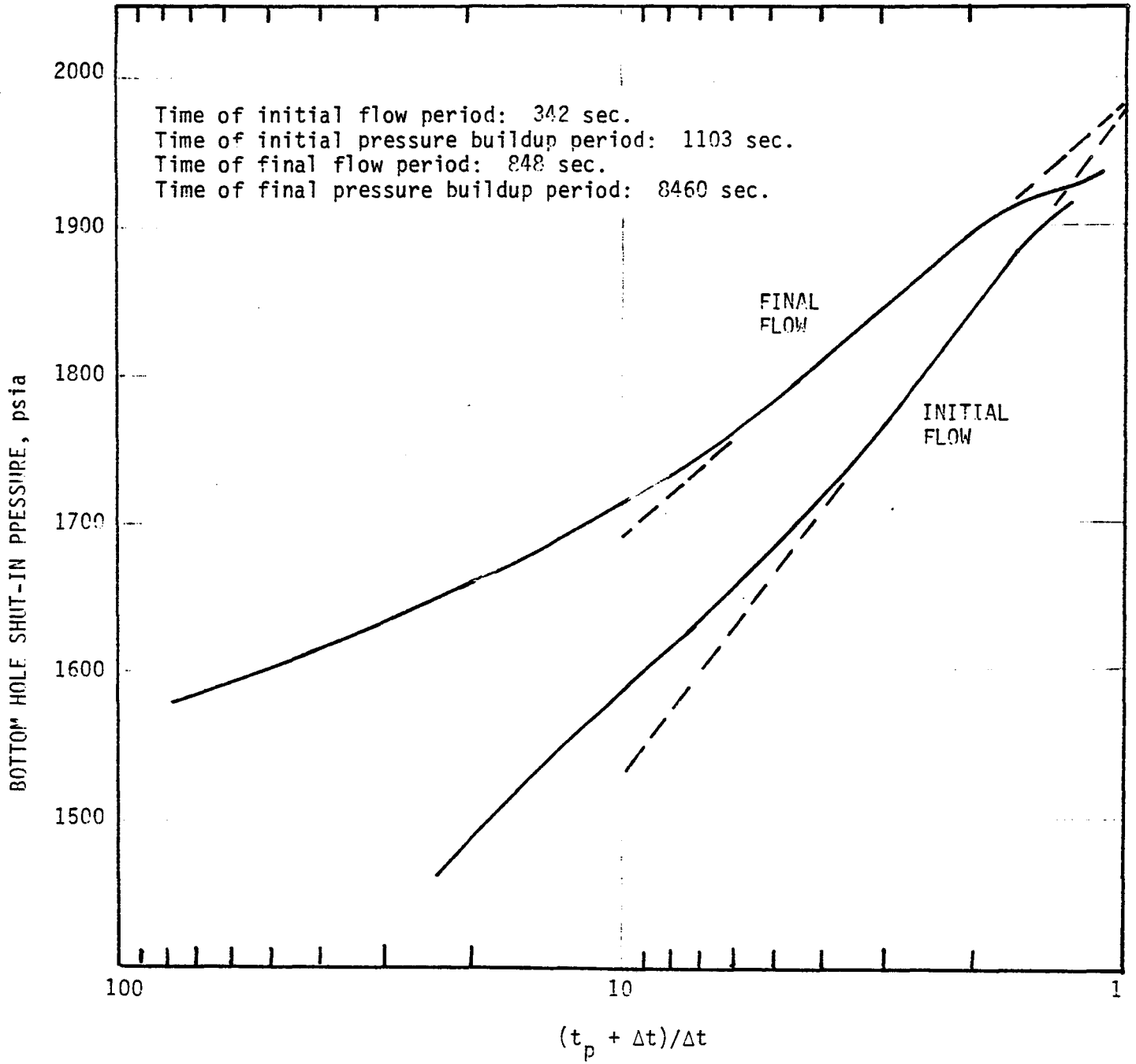


Figure 7. Horner plot of data from drillstem test 2680-1

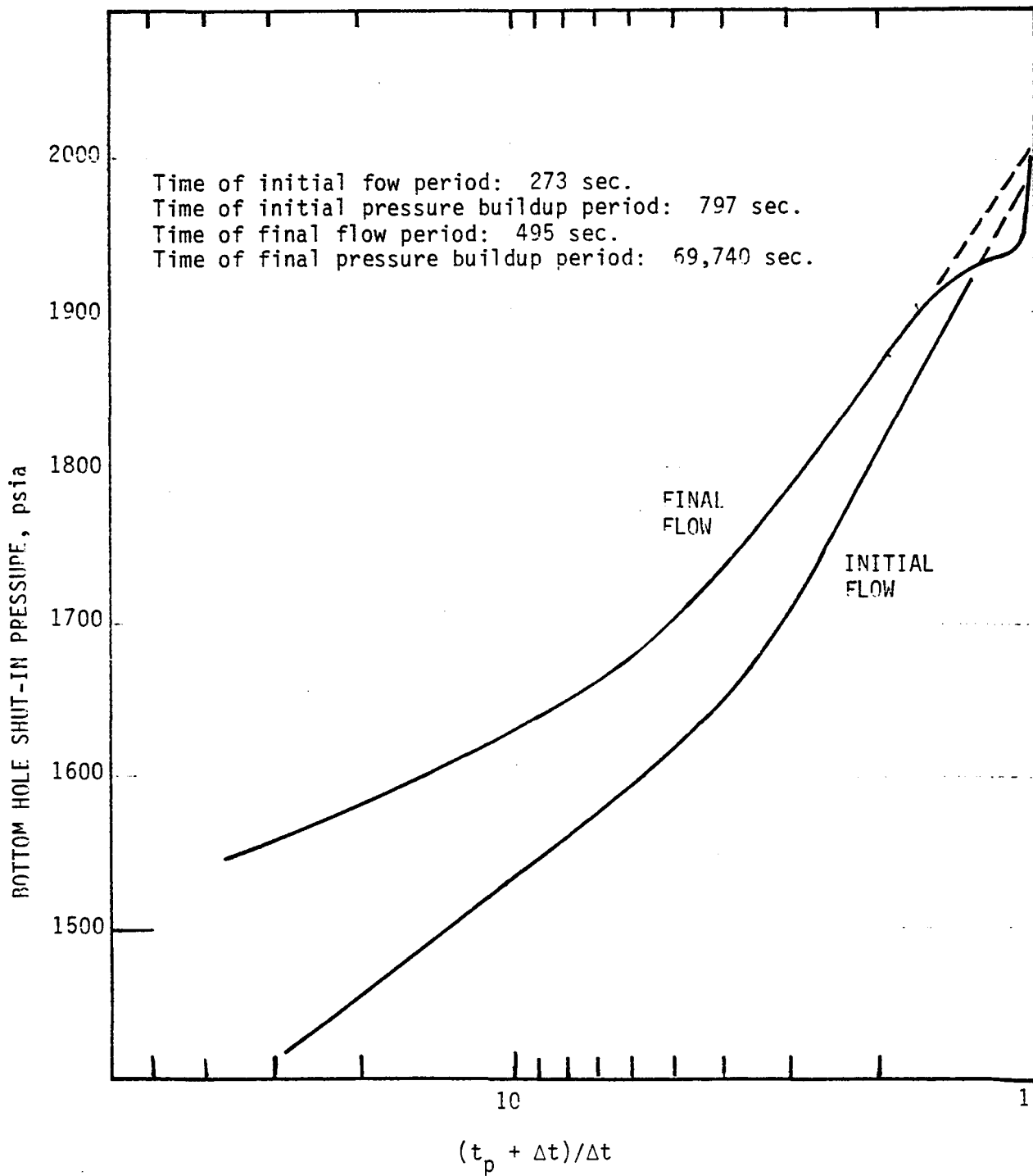


Figure 8. Horner plot of data from drillstem test 2680-2.

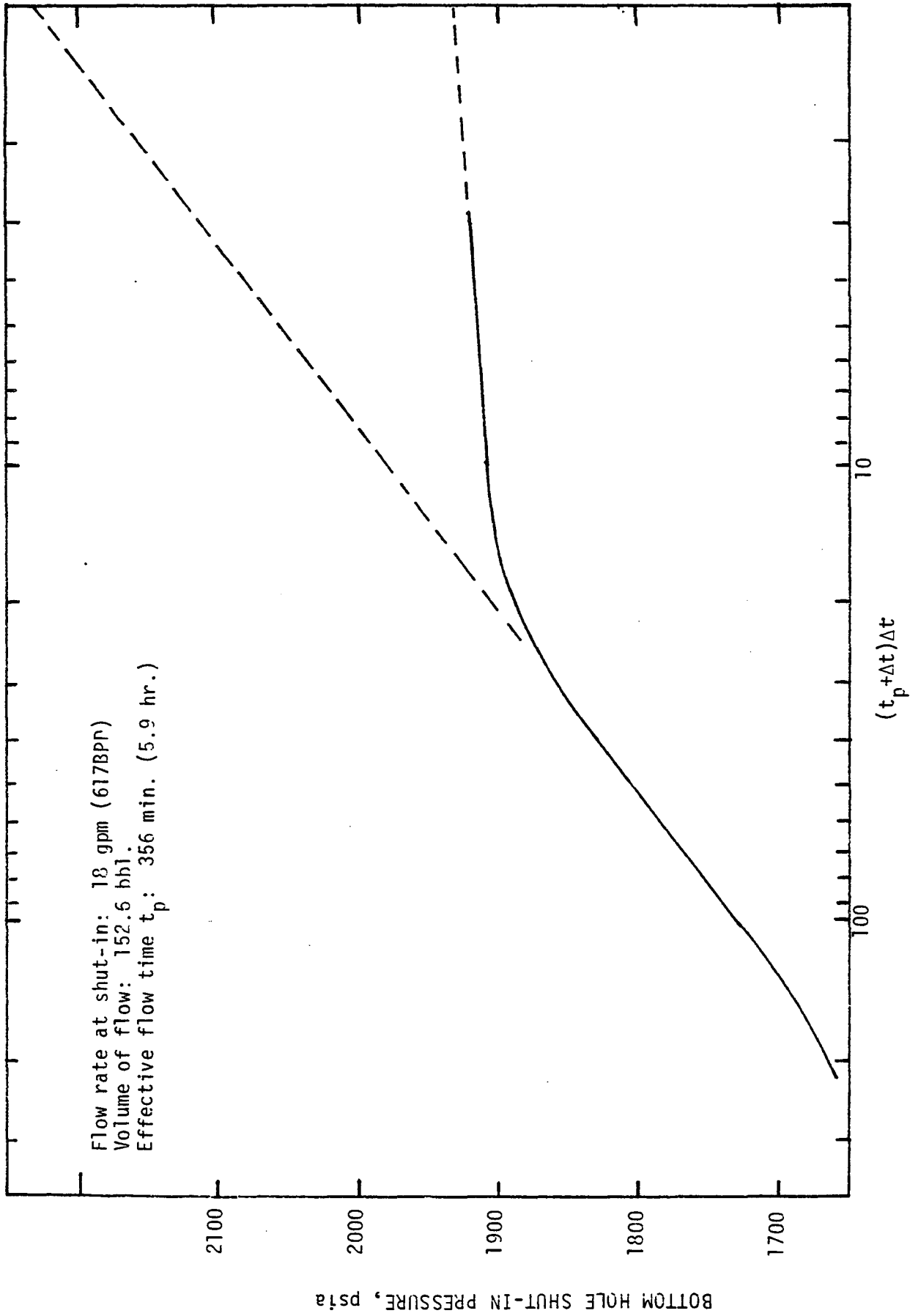


Figure 9. Horner plot of pressure-buildup data following flow test #1.

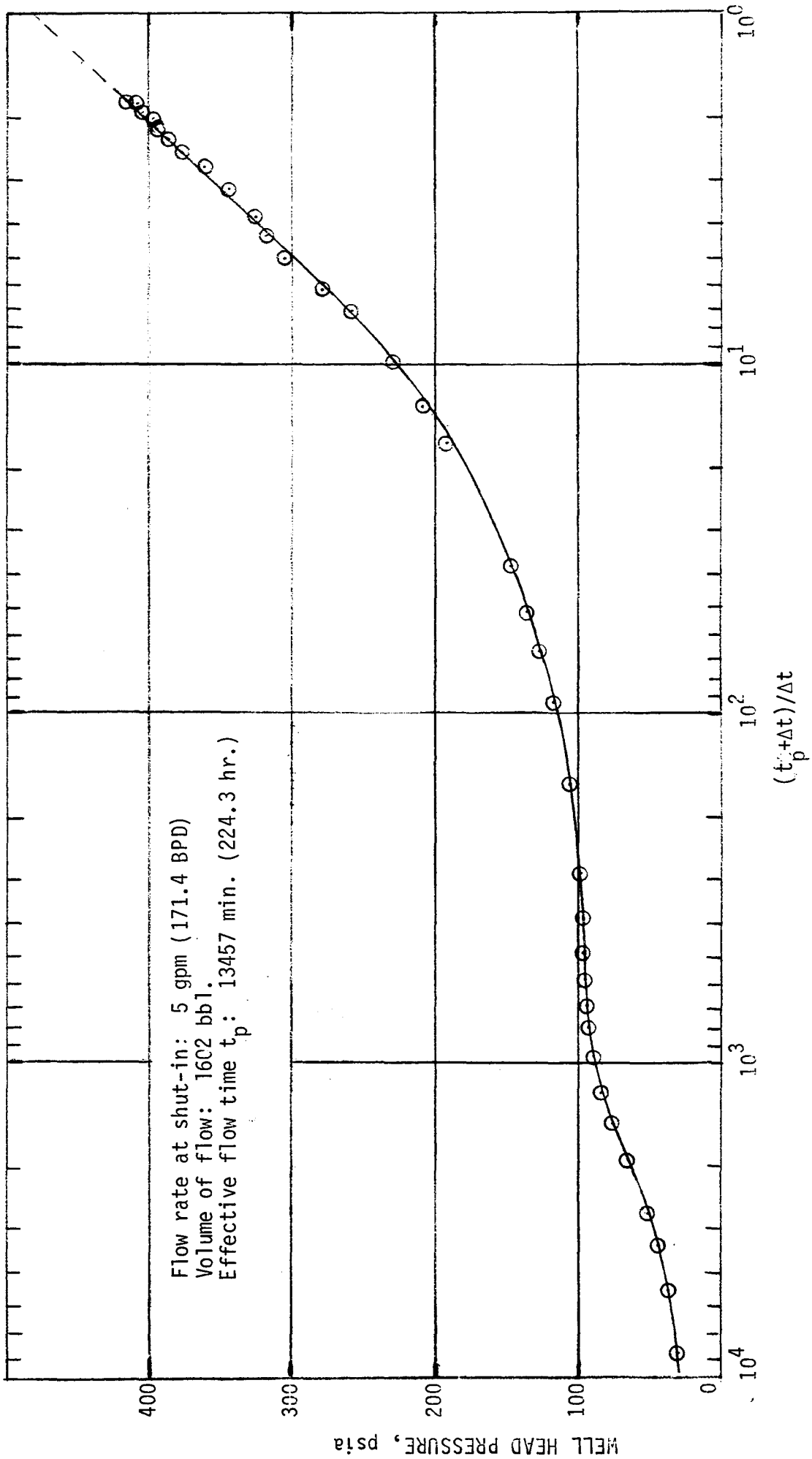


Figure 10. Horner plot of pressure-buildup data following flow test #2.

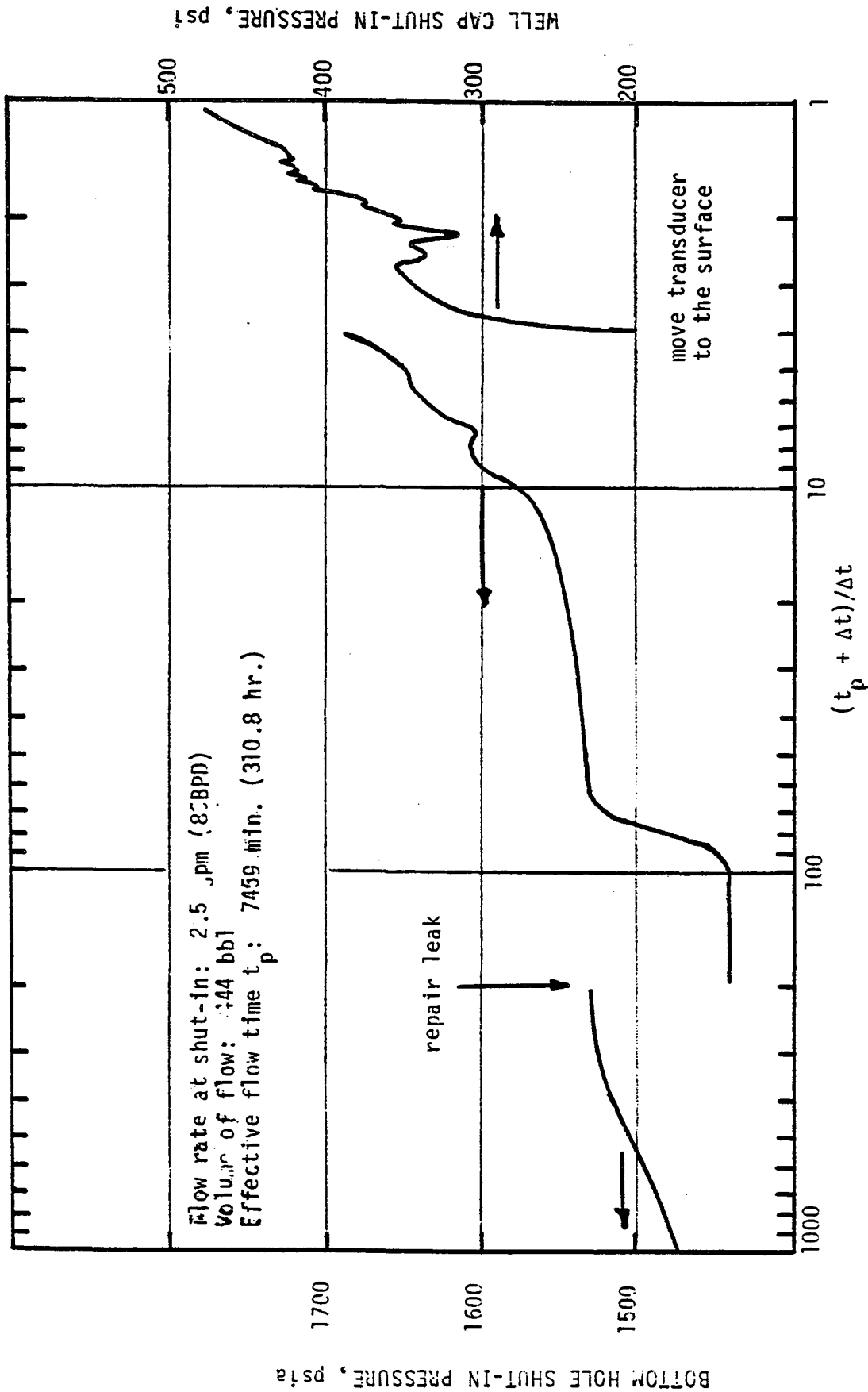


Figure 11. Horner plot of pressure-buildup data following flow test #3.

Table I. Permeability values for ERDA-6 deduced from pressure build-up data

| Test | q ⁽¹⁾ (bbl/d) | m ⁽²⁾ (psi/cycle) | kh/μ (md-ft/cp) | k ⁽³⁾ md |
|--------------------|-----------------------------|---------------------------------|--------------------|------------------------|
| DST 2680-1 initial | 1175 | 450 | 425 | 13.3 |
| DST 2689-1 final | 744 | 295 | 410 | 12.8 |
| DST 2680-2 initial | 1418 | 630 | 366 | 11.5 |
| DST 2680-2 initial | 1017 | 480 | 345 | 10.8 |
| Flow test #1 | 617 | 260 | 385 | 12.0 |
| Flow test #2 | 171 | 280 | 99 | 3.1 |
| Flow test #3 | 86 | 300 | 47 | 1.5 |

(¹) estimated from data in reference 1.

(²) estimated from figures 7, 8, 9, 10, and 11.

(³) effective height = 56.5 ft., i.e., distance between bottom of packer a contact between anhydrite II and halite I. Viscosity of brine = 1.77 cp.

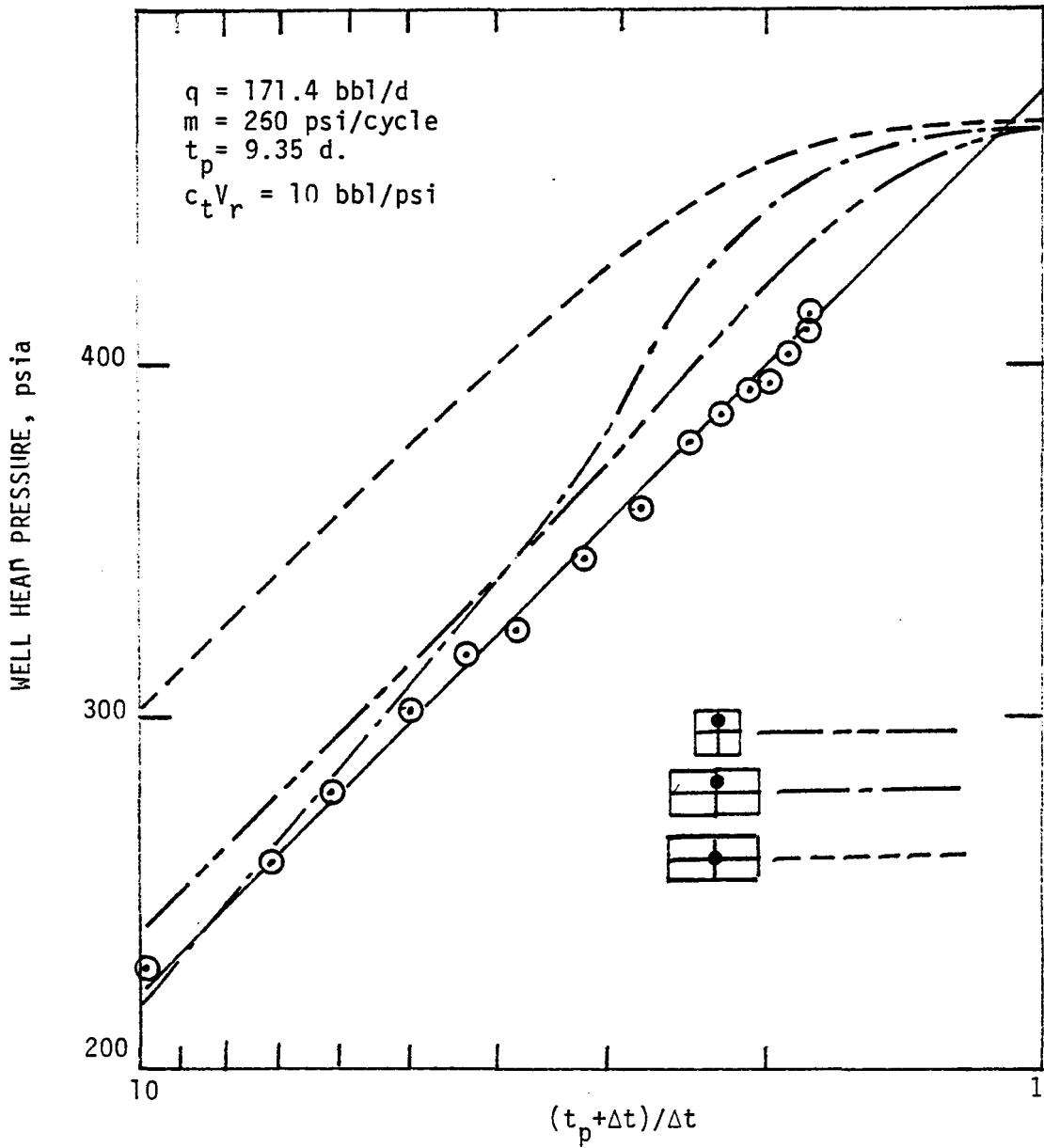


Figure 12. Horner plot of shut-in pressure for ERDA-6 following flow test #2. The circles are selected data points. The dashed lines are theoretically calculated pressure buildups for the geometries indicated and for the values listed in the left hand corner.

The geometry of the reservoir is contained in the terms C_A and P_{DMBH} which are available in tables or in graphs (refs. 2, 3). For this example, The best fit suggests that ERDA-6 is located off center of a symmetric reservoir with a $c_t V_r$ value of about 10 bbl/psi. A few other examples were also attempted but the best fits were obtained for $c_t V_r$ values around 10 bbl/psi.

2.4 Flow Data

The flow data does not indicate a two-porosity system as clearly as the pressure buildup data primarily because the flow tests could not be run long enough. The flow rates versus time for all three flow tests are summarized in Figures 13 and 14. In flow test #2, the flow rate at first increased because of the discharge of heavy drilling mud. Techniques for analyzing constant drawdown flow rate data for two-porosity systems have only been published recently (ref. 4). A summary is presented in appendix A. The dimensionless flow rate versus dimensionless time is as illustrated in Figure 15 and is characterized by three parameters; r_{eD} , the dimensionless outer boundary and radius; F_{ft} , the dimensionless fracture storage parameter; ϵ , the dimensionless matrix/ fracture permeability ratio. The curve shown in figure 16 is essentially a sum of two exponential terms. The data in Figures 13 and 15 only indicates the early part of the curve or only the first of the two exponential terms. It yields information on the dimensionless fracture storage parameter.

In the appendix A, it is shown that the product of compressibility and volume for the first porosity is given by

$$(c_t V_r)_f = 1.44 q(0) T_{1/2} / (p_i - p_{wf}) \quad (4)$$

About 150 bbl had flown prior to flow test #2. Hence it will be assumed that the reservoir had been unperturbed. The following parameters apply to flow test #2: $q(0) = 30$ gpm; $T_{1/2} = 2000$ min., $p_i - p_{wf} \approx 600$ psi. Hence, $(c_t V_r)_f \approx 3.4$ bbl/psi. Flow test #3 was started before the reservoir had stabilized from the perturbation of flow test #2. Hence, a correct value for $p_i - p_{wf}$ is not readily available and the data cannot be used to estimate

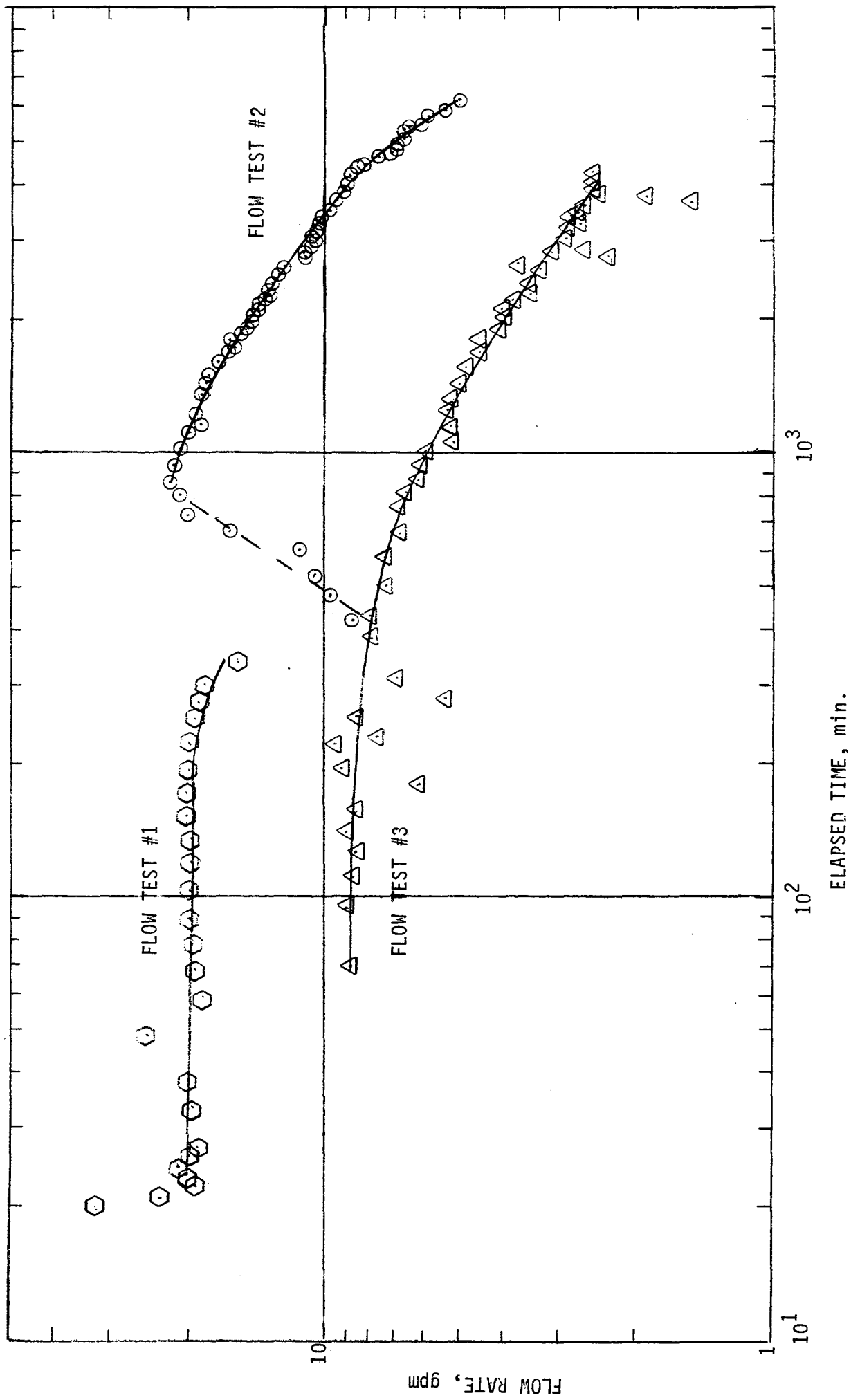


Figure 13. Log-log plot of flow rate versus time for the three flow tests at ERDA-6.

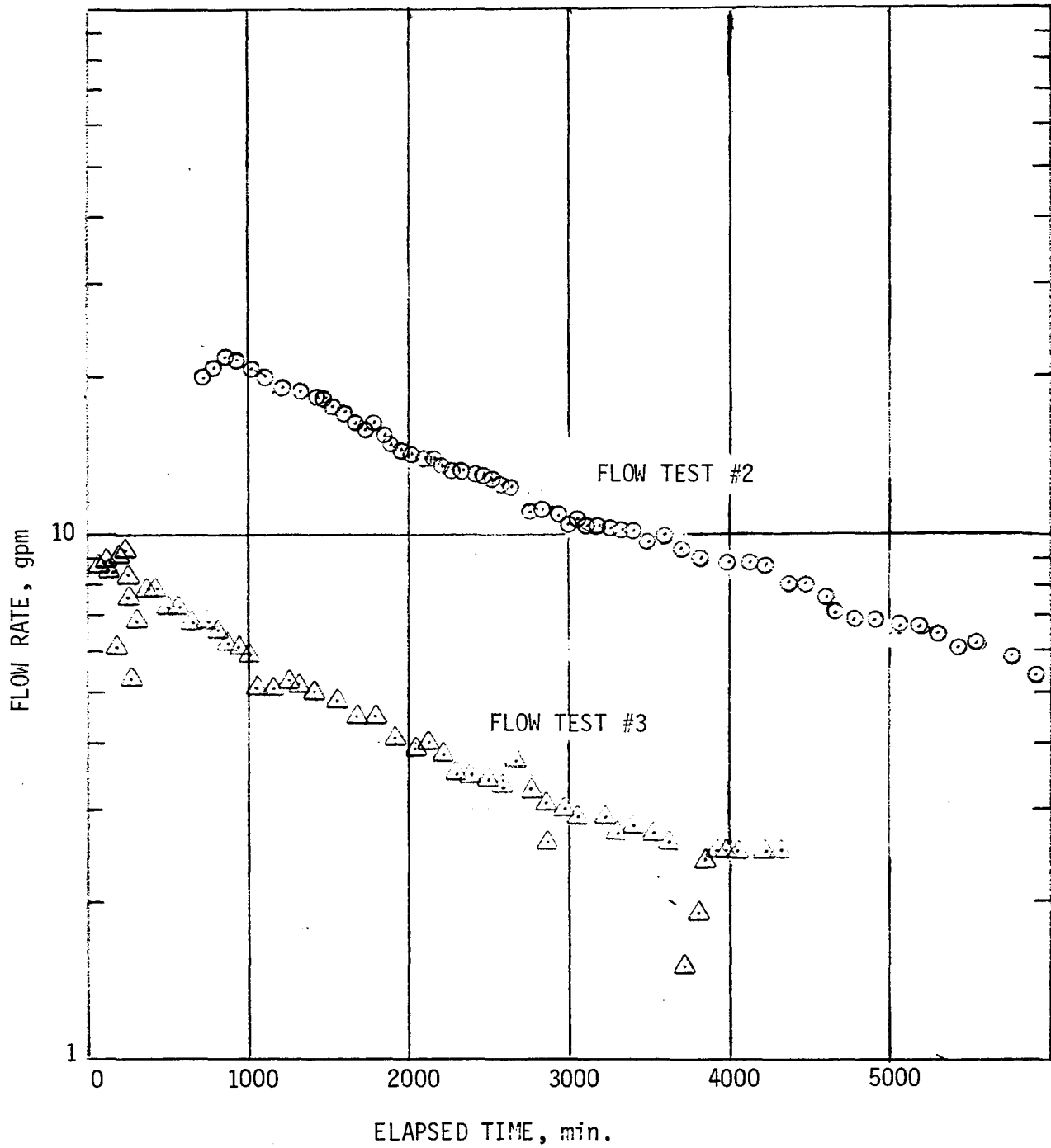


Figure 14. Semilog plot of flow rate versus time for flow tests #2 and #3 at ERDA-6.

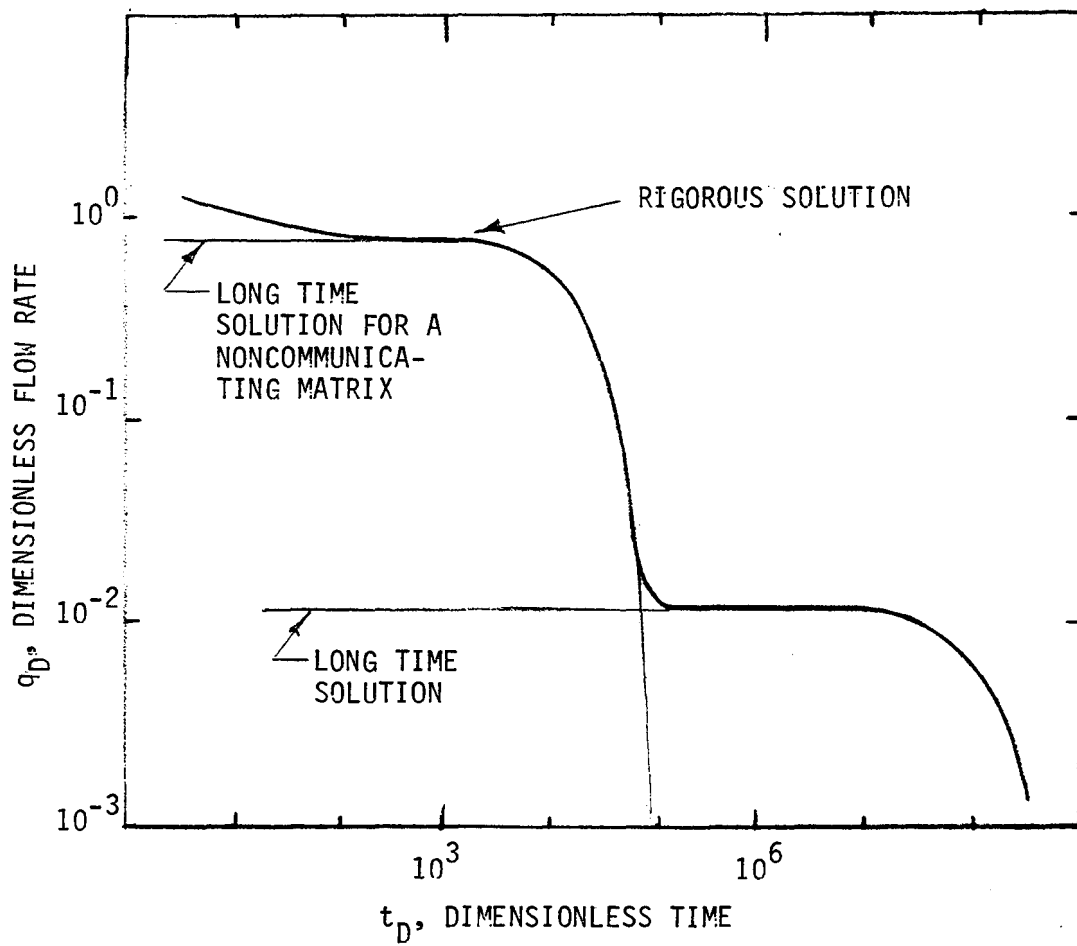


Figure 15. Dimensionless flow rate versus dimensionless time for constant drawdown test.

$(C_t V_R)_f$. It will be shown in section 4.2 that $C_t V_R$ is about 15 bbl/psi. Hence, the data indicate that the brine stored in the fracture volume is much less than the brine stored in the matrix volume.

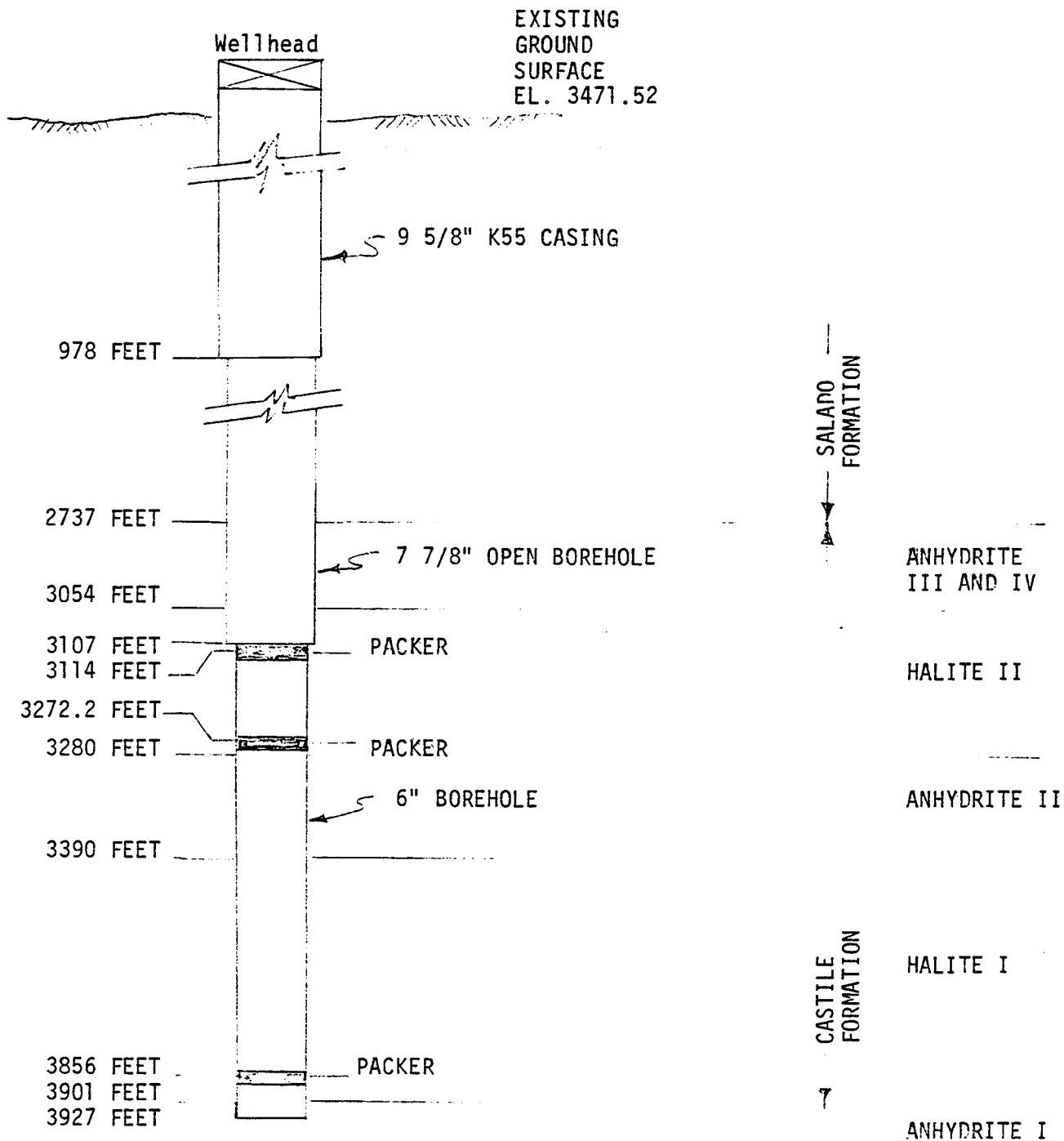
3 REDUCTION AND ANALYSIS OF WIPP-12 DATA

3.1 Geologic profile of WIPP-12

The dimensions and geologic profile of the WIPP-12 borehole are presented in Figure 16. The location of the three packer assemblies inserted into the borehole prior to shut-in on 1/5/82 is also shown in Figure 16. The location of the main fracture is based on coring data, well logging data, downhole images from an acoustical televiewer, and a spinner log. Figure 17 shows the densilog and the compensated neutron log. Both logs indicate a signal between 3010 and 3020 feet but the maximum porosity is only 1% on the neutron log. As in ERDA-6, the fracture was intercepted near the bottom of the anhydrite layer, which at WIPP-12 is 320 feet thick. Figure 18 shows the image of the acoustical televiewer while Figure 19 shows the spinner log. The sonic televiewer shows a 6 feet crack while the spinner log clearly shows that most of the flow comes from this crack. The spinner log also indicates a small inflow 40 feet below the main crack. The acoustical televiewer also indicates small fractures in this area as shown in Figure 20.

3.2 Reservoir Testing Activities

The techniques employed to acquire hydrologic data at WIPP-12 were the same as those used at ERDA-6, namely, DST and flow testing with associated subsequent pressure buildup testing. However, the flow testing activity was delayed until May, 1982, for after encountering brine at the 3010 to 3020 feet level the hole was further cored to depth of 3925 feet. During the coring activities, 59,006 barrels of brine flowed to the surface. The outflow of brine is summarized in Figure 21. Because of this large loss of brine, hydrologic testing could not be done following the coring activities. The well was shut-in on January 5, 1982 and the reservoir was allowed to equilibrate in pressure. Pressure was monitored at the well head during the



1. DEPTH OF DOWNHOLE COMPONENTS WITH REFERENCE TO GROUND SURFACE.
2. DEPTHS GIVEN FOR PACKERS INDICATE THE CENTER OF THE RUBBER ELEMENT.
3. GEOLOGIC PROFILE FROM FREELAND AND DADOURIAN, GEOLOGIC DATA FOR BOREHOLE WIPP-12, D'APPOLONIA CONSULTING ENGINEERS, 1982, UNPUBLISHED REPORT.

Figure 16. Geological profile and borehole configuration for WIPP-12. The dark areas indicate the location of three packers inserted prior to shut-in on 1/5/82. Figure taken from Reference 1.

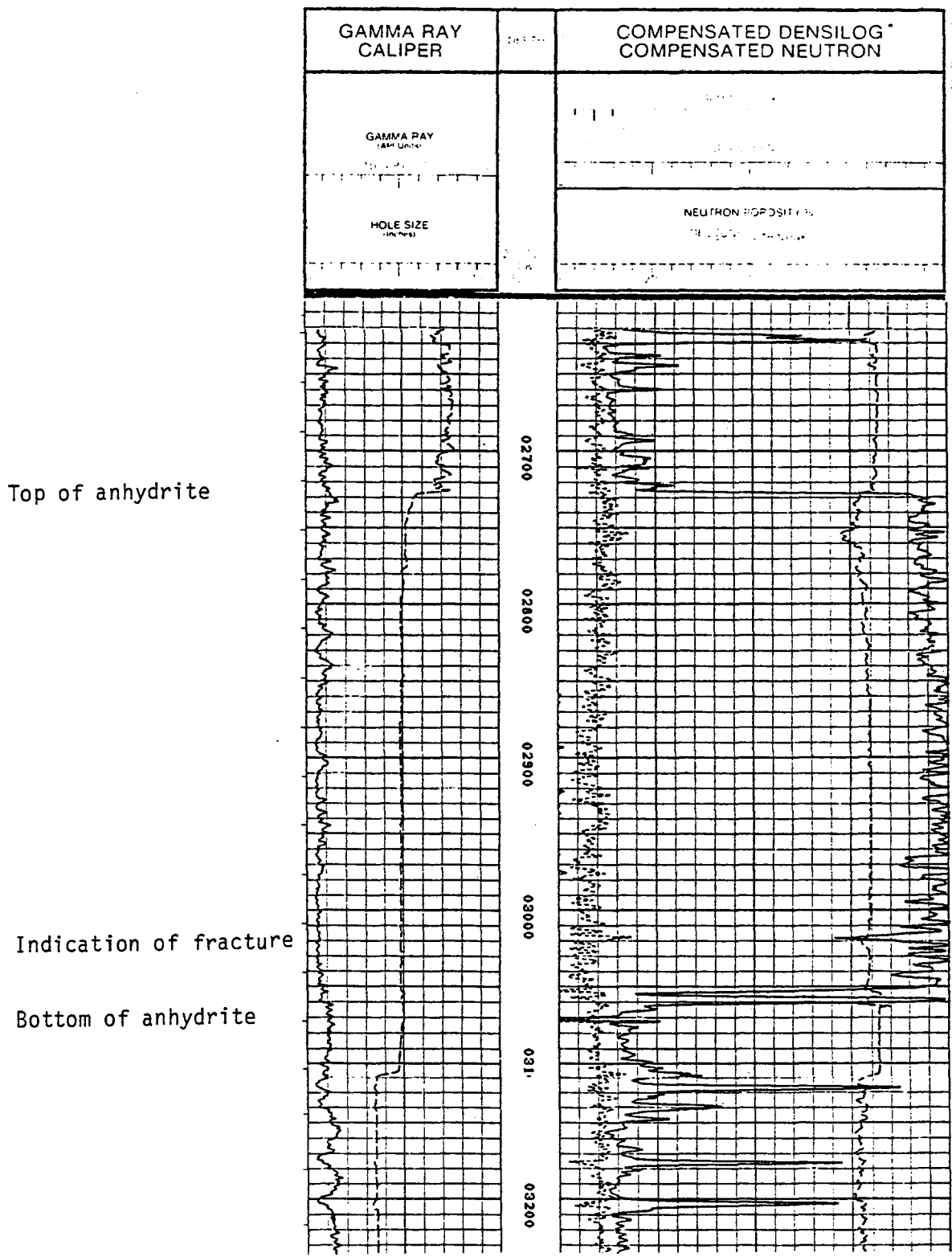


Figure 17. Densilog and compensated neutron log for WIPP-12. Figure taken from reference 1.

Top of
fracture

Bottom of
fracture

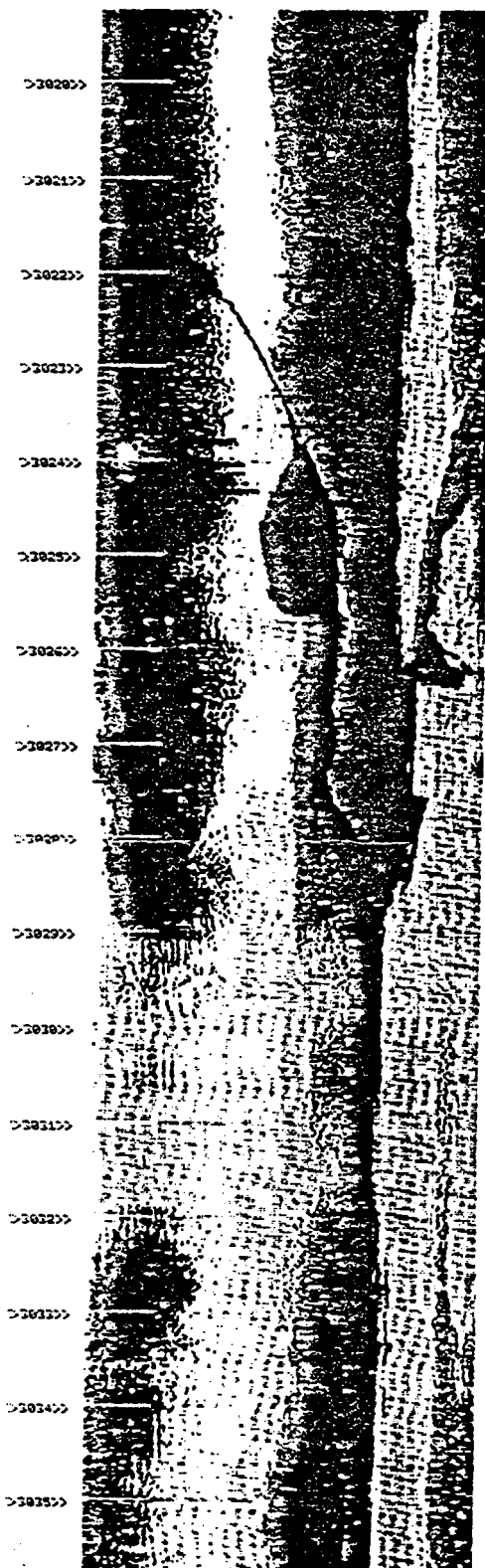


Figure 18. Acoustical image of fracture obtained with the acoustical televiewer. Figure taken from reference 1.

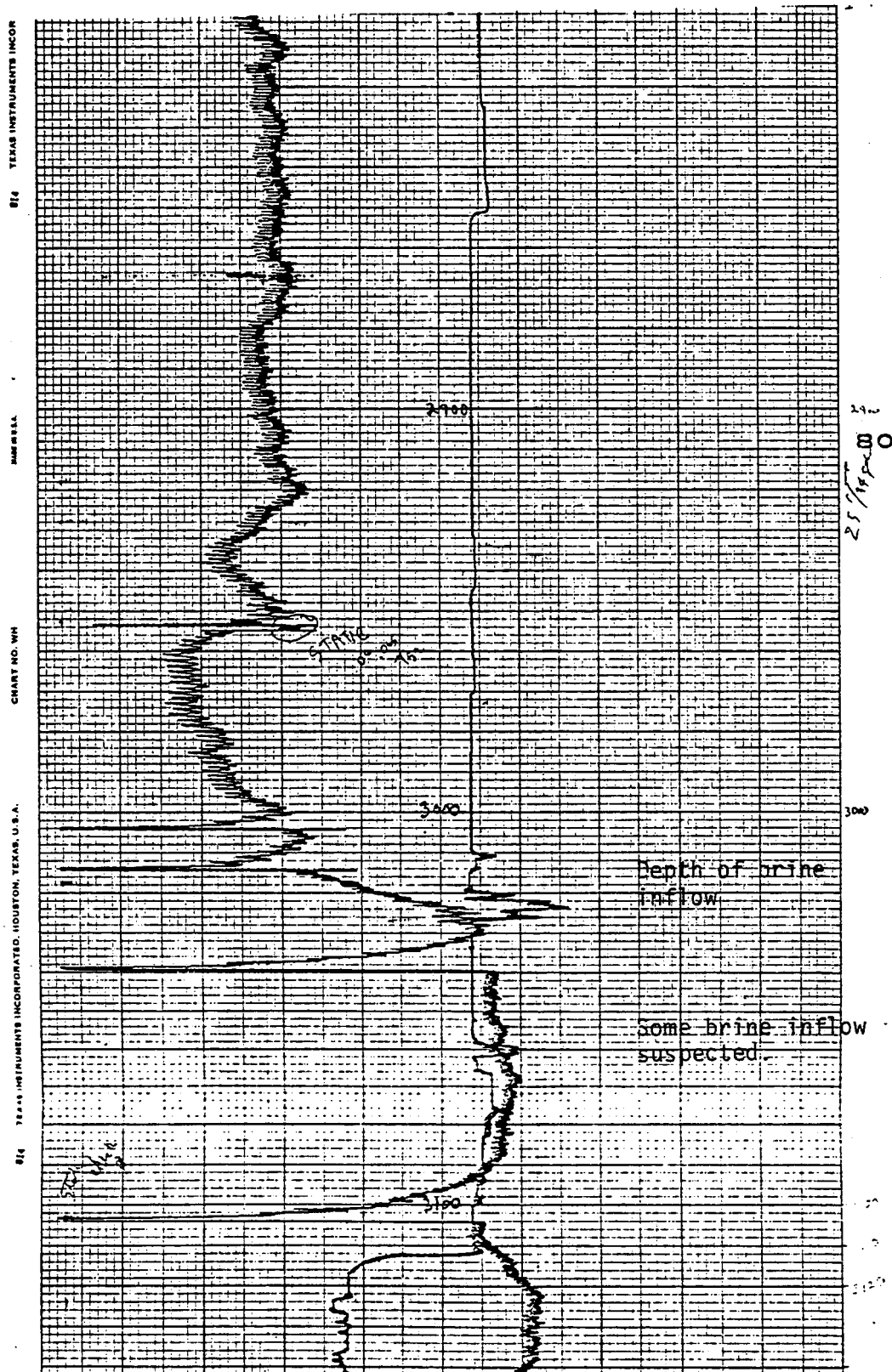


Figure 19. Spinner log from WIPP-12. Figure taken from reference 1.

Indication
of small
fractures.

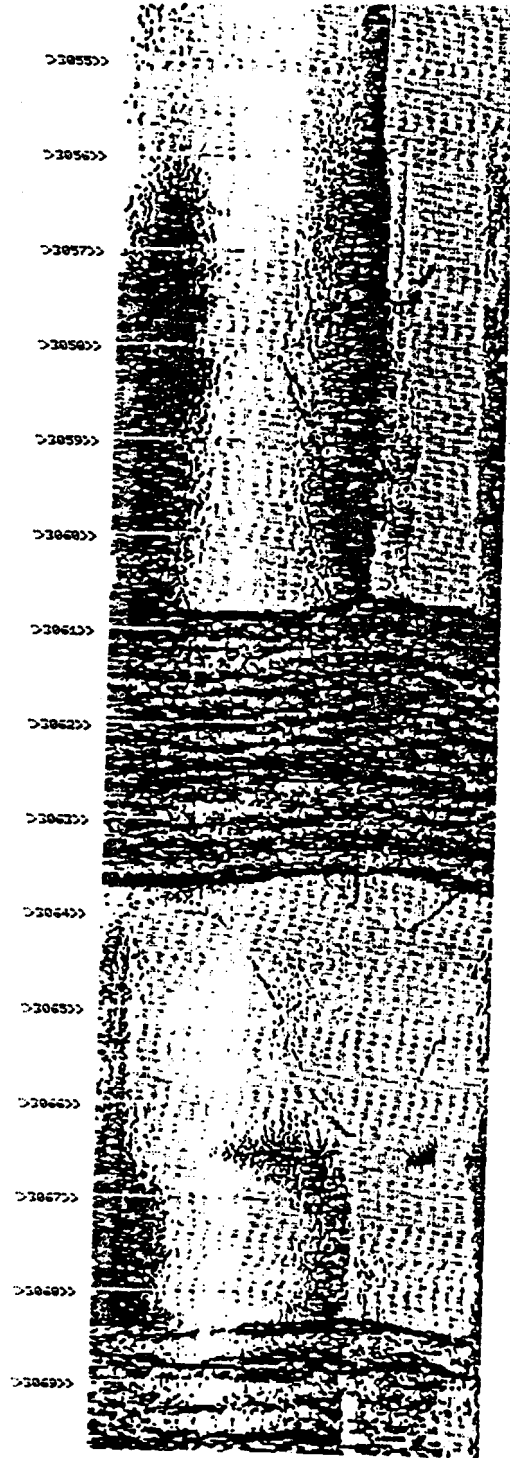


Figure 20. Image of suspected area of inflow obtained with the acoustical televiwer. Figure taken from reference 1.

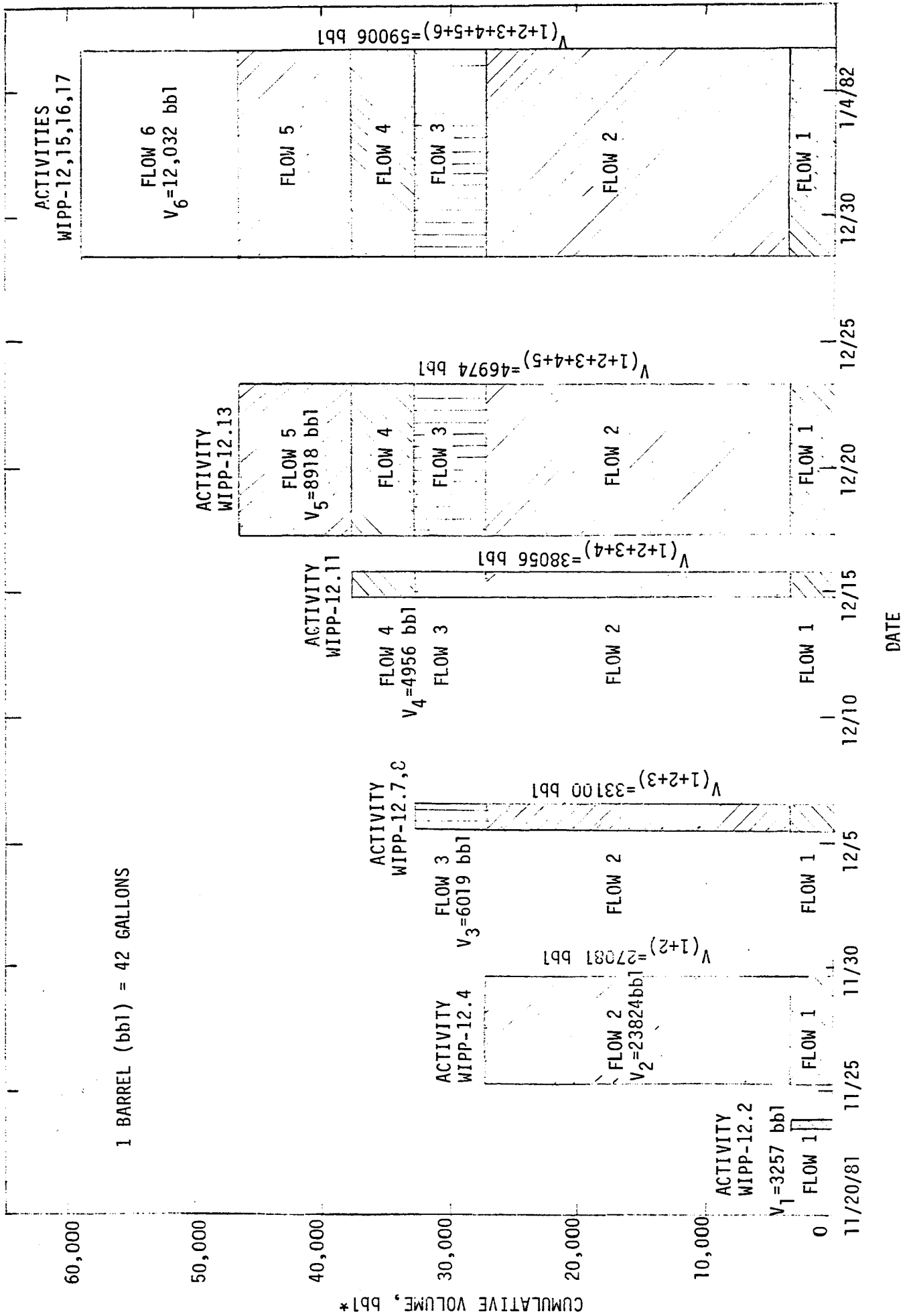


Figure 21. Summary of flow activities during coring at WIPP-12. Figure taken from Reference 1.

reequilibration period, which lasted until the end of April 1982. Prior to shut-in, three packers were installed to isolate the geologic formation. The location of the packers are shown in Figure 16.

The arrangements for the DSTs is shown in Figures 22 and 23. The DSTs were performed prior to the acoustical televiewer logging and thus prior to an understanding that the brine came from the large fracture. The Lynes packer assembly was the same as that used at ERDA-6. The 3020 DSTs each consisted of one flow period and one pressure buildup period. The 2986 DSTs consisted of two flow periods each followed by a pressure buildup period. However, the second flow period always resulted in flow at the surface.

Two flow tests were performed between May 20, 1982 and June 2, 1982. The first flow test was a short term test known as flow test #2. The well was allowed to discharge at a constant downhole pressure of 1740 psia for about 5 hours. 94,845 gal. (2,258 bbl) of brine discharged over the flowing time interval. Discharge rates were monitored at the surface while the pressure was monitored downhole and at the wellhead. Following shut-in, the downhole pressure was monitored for about 20 hours.

Flow test #3 was a long term test. The well was allowed to discharge 1,041,599 gal. (24,800 bbl) over a period of about 11 days. Discharge rates and pressure were monitored at the wellhead. Although downhole pressure was not measured, it is believed the test was effectively a constant pressure drawdown-variable discharge rate flow test. During the course of the flow period, salt crystalized within this pipe and blocked flow from the well. To alleviate this problem, a by-pass flow line was constructed from a fire hose that allowed the entire discharge system to be periodically flushed with fresh water to remove salt blockage. Before shut-in, a Johnston-Macco downhole pressure and temperature transducer was lowered to a depth of 3020 feet. Following shut-in the pressure was monitored downhole and at the wellhead for a period of over 2 months.

3.3 Pressure Buildup Data

Figure 24 shows Horner plots of the early DST data. No permeability

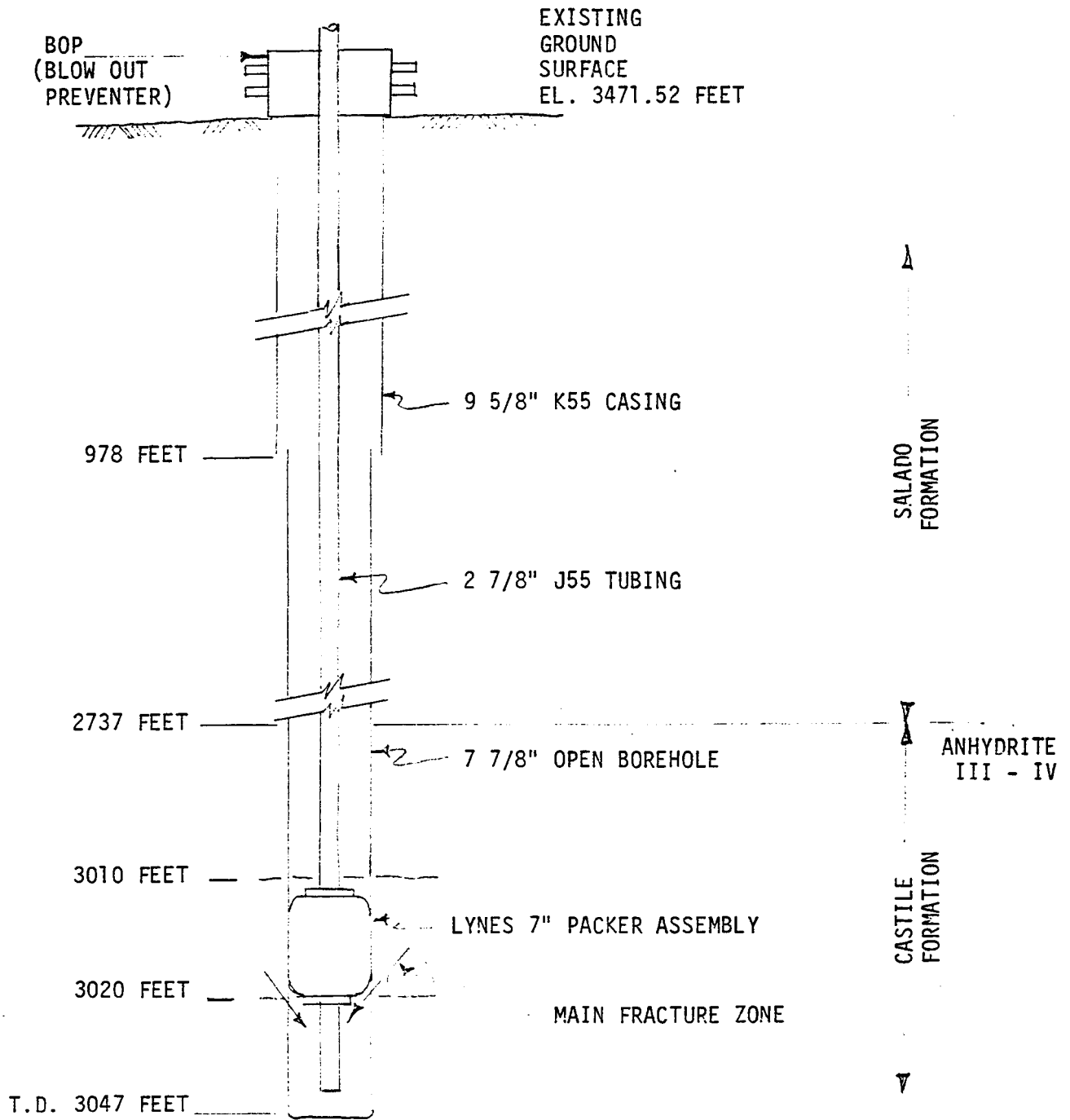


FIGURE NOT TO SCALE

1. DEPTH OF DOWNHOLE COMPONENTS WITH REFERENCE TO GROUND SURFACE.
2. GEOLOGIC PROFILE FROM FREELAND AND DADOURIAN, GEOLOGIC DATA FOR BOREHOLE WIPP-12, D'APPOLONIA CONSULTING ENGINEERS, 1982, UNPUBLISHED REPORT.

Figure 22. Drillstem test configuration for WIPP-12.
Figure taken from Reference 1.

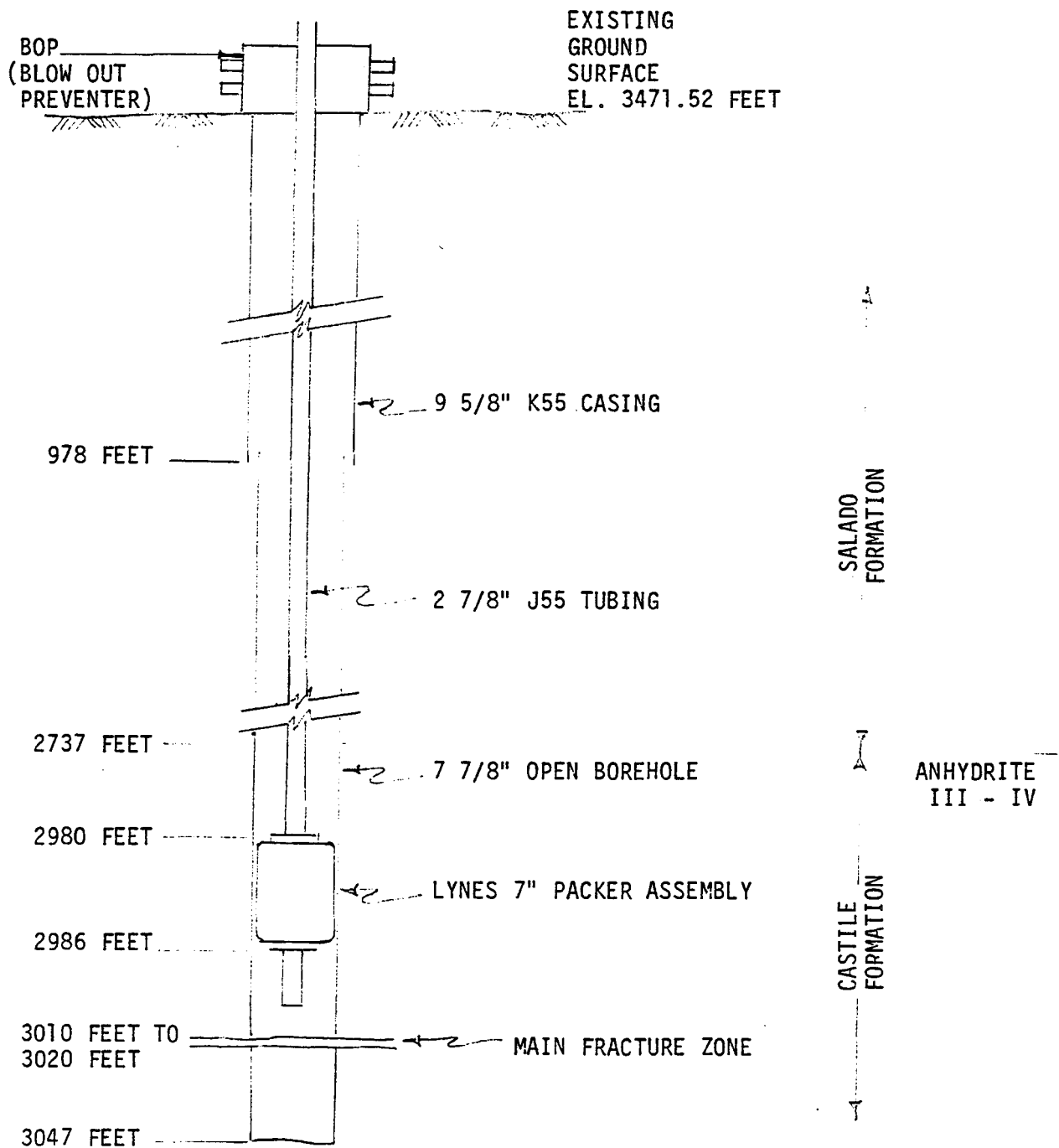


FIGURE NOT TO SCALE

1. DEPTH OF DOWNHOLE COMPONENTS WITH REFERENCE TO GROUND SURFACE.
2. GEOLOGIC PROFILE FROM FREELAND AND DADOURIAN, GEOLOGIC DATA FOR BOREHOLE WIPP-12, D'APPOLONIA CONSULTING ENGINEERS, 1982, UNPUBLISHED REPORT.

Figure 23. Drillstem test configuration for WIPP-12.
Figure taken from Reference 1.

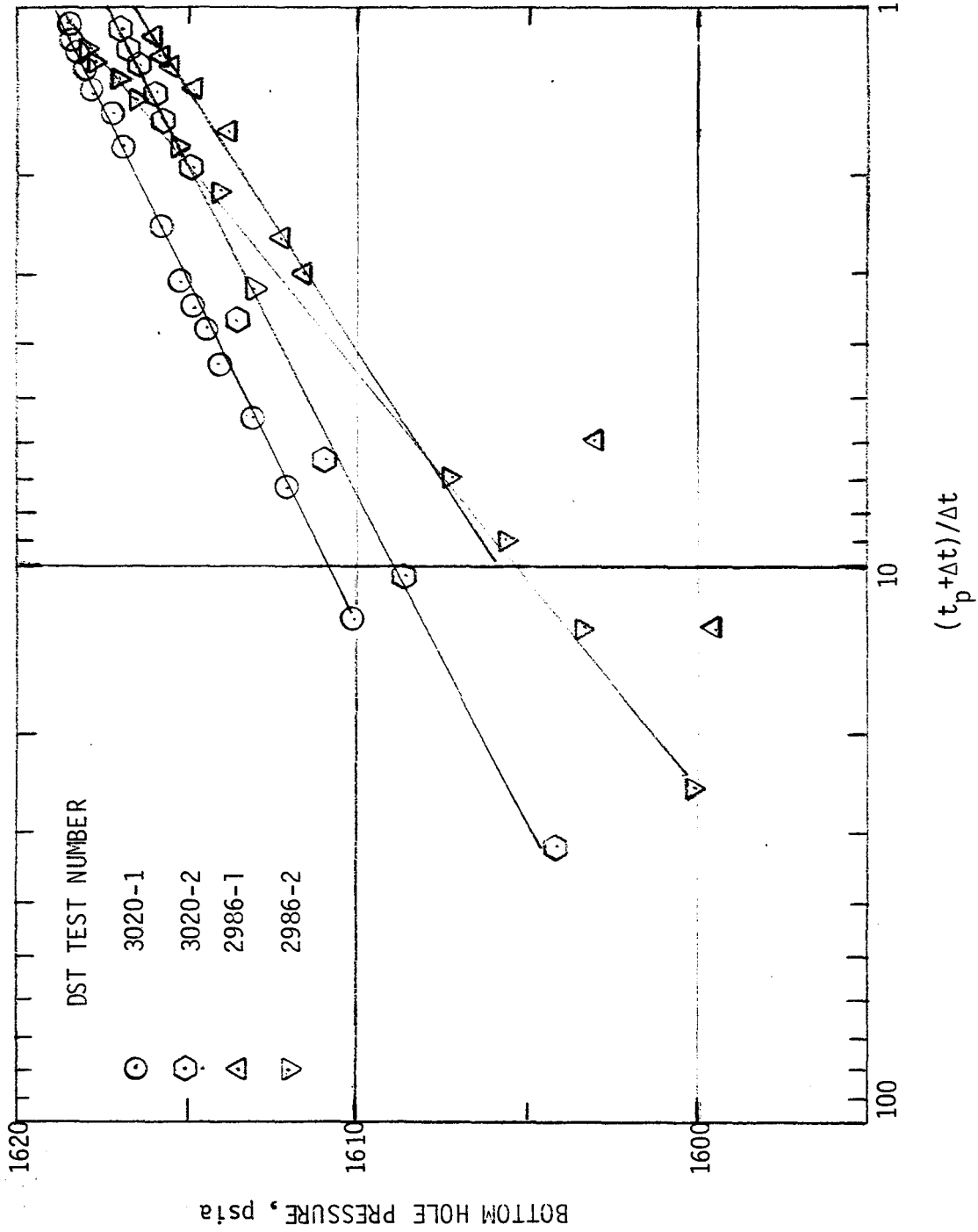


Figure 24. Horner plots of drillstem test data from WIPP-12.

calculations were attempted since it is not clear that pressure buildups are the result of radial flow in either the large crack or in the reservoir. Figure 25 is a Horner Plot of the pressure buildup following flow test #2, which was performed on May 20, 1982. The plot is typical of the buildup curve for a naturally fractured reservoir of the two porosity type. The parameters characterizing the reservoir can be evaluated from the two parallel semilog straight lines using a method proposed by Udrih and Ersaghi (see Appendix A). The results are $kh/\mu = 67.5$ darcy-ft/cp, $F_{ft}=0.941$, and $E/[(\phi c_t)_f + (\phi c_t)_{ma}] = 0.0121$.

Figure 26 and 27 are plots of the well head and bottom hole pressures following shut-in on January 5, 1982 and June 2, 1982. Figure 28 is a square-root plot of the same data. The curves show linear flow for the first ten days, an indication that the fracture is very long. Figure 29 is a Horner plot of the pressure buildup data following flow test #3 and theoretical calculations using parameters in the left-hand corner of the figure and equations 3 and 4 of section 2.3 of this report. For this example, the curve suggest that WIPP-12 is located at the center of a square or circular reservoir with a $c_t V_r$ value near 1000 bbl/psi (the P_{DMBH} curve for a circle is almost the same as that of a square). A few other examples were also attempted but the best fits were obtained for $c_t V_r$ values around 1000 bbl/psi.

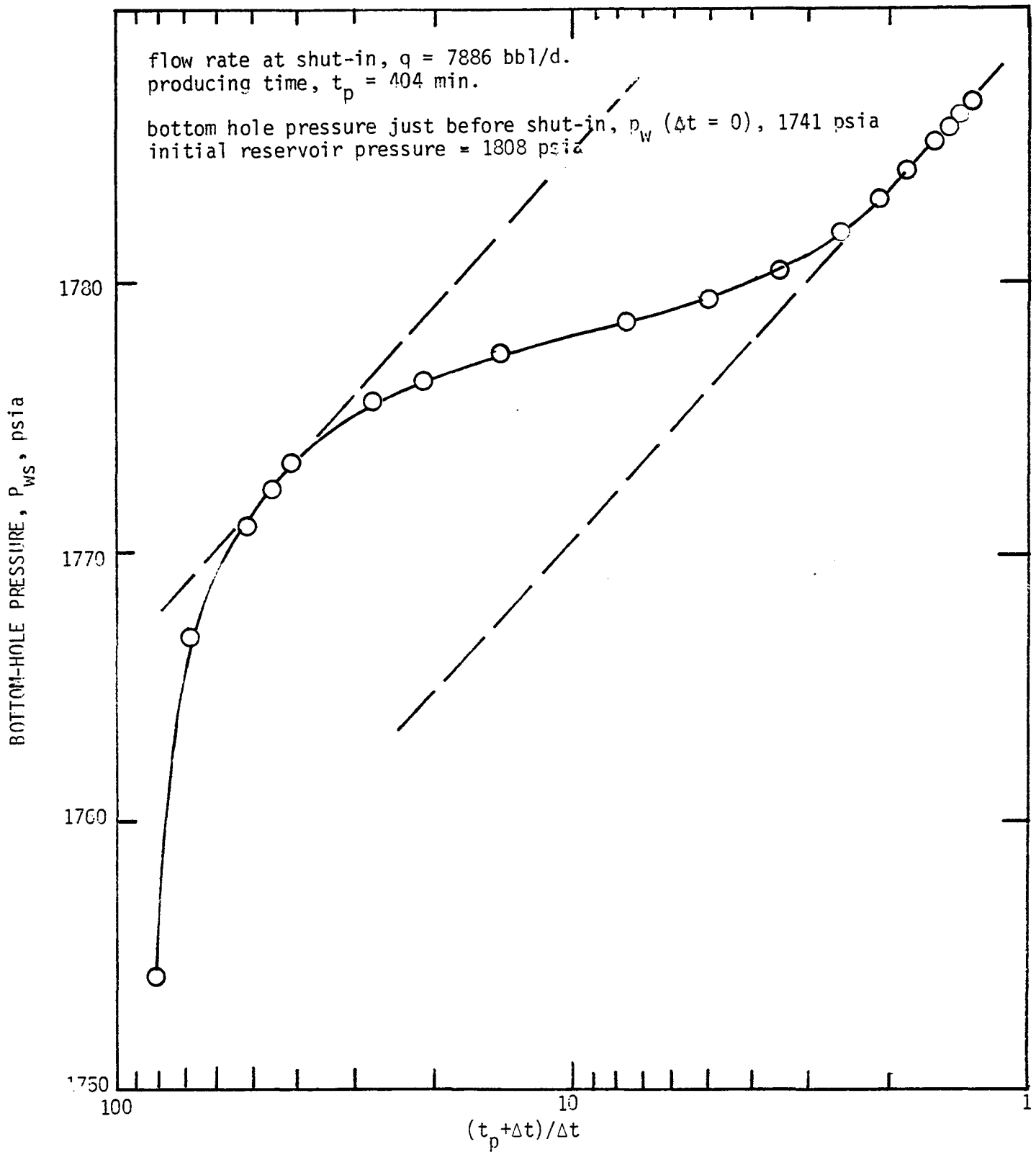


Figure 25. Horner plot of pressure buildup following flow test #2 of WIPP-12.

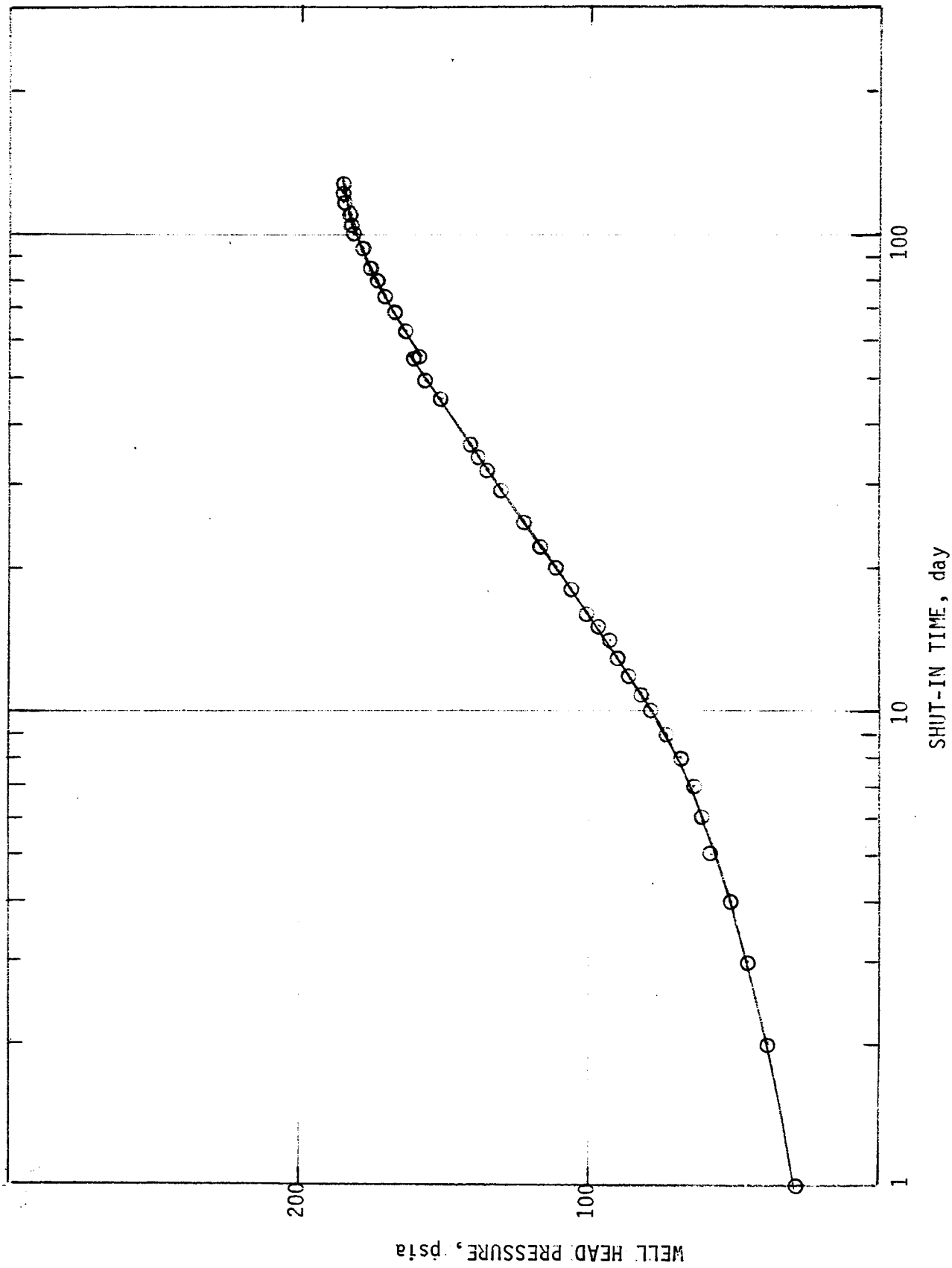


Figure 26. Pressure buildup at WIPP-12 following shut-in on 1/5/82

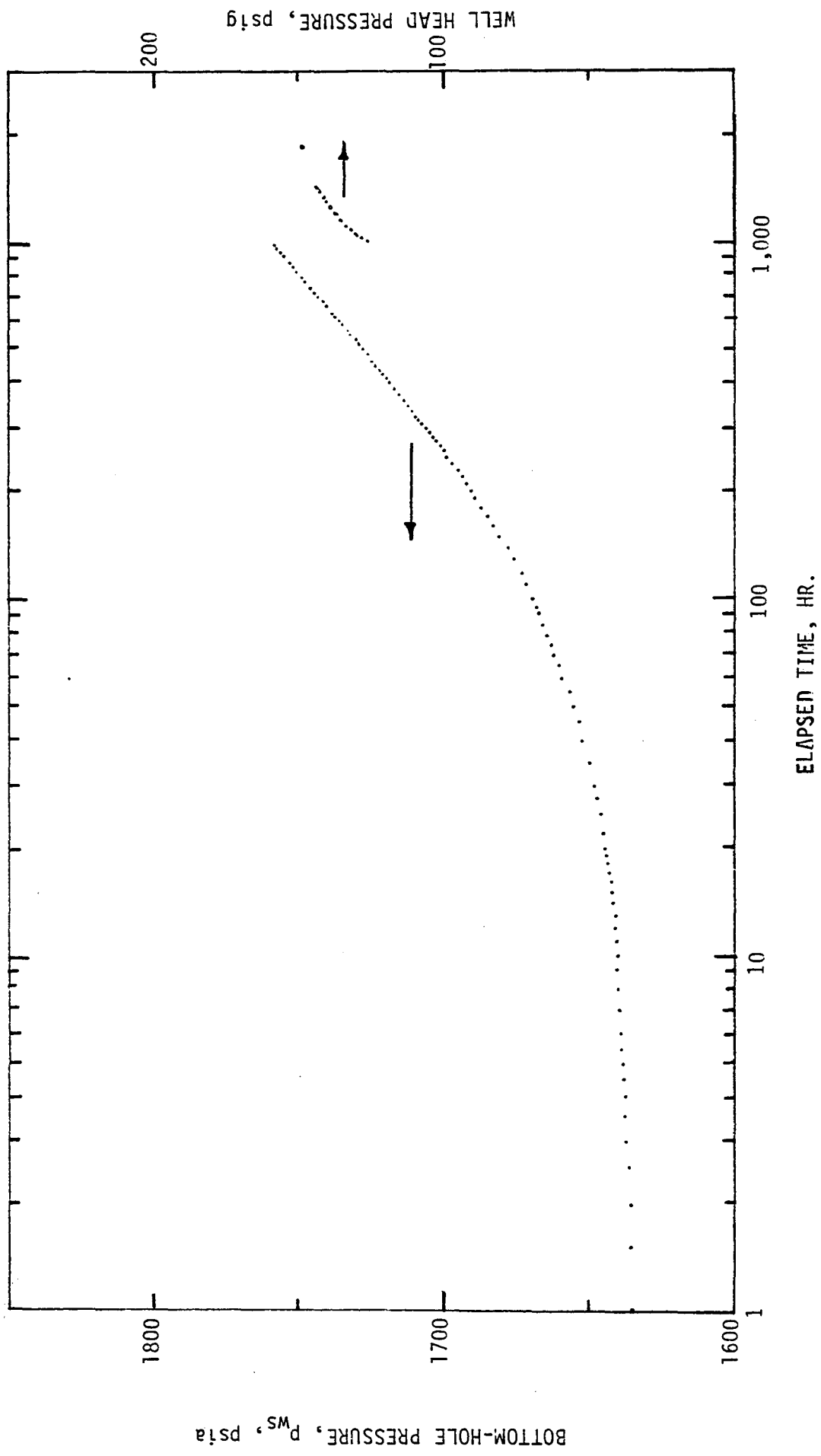


Figure 27. Pressure buildup at WIPP-12 following shut-in on 6/2/82.

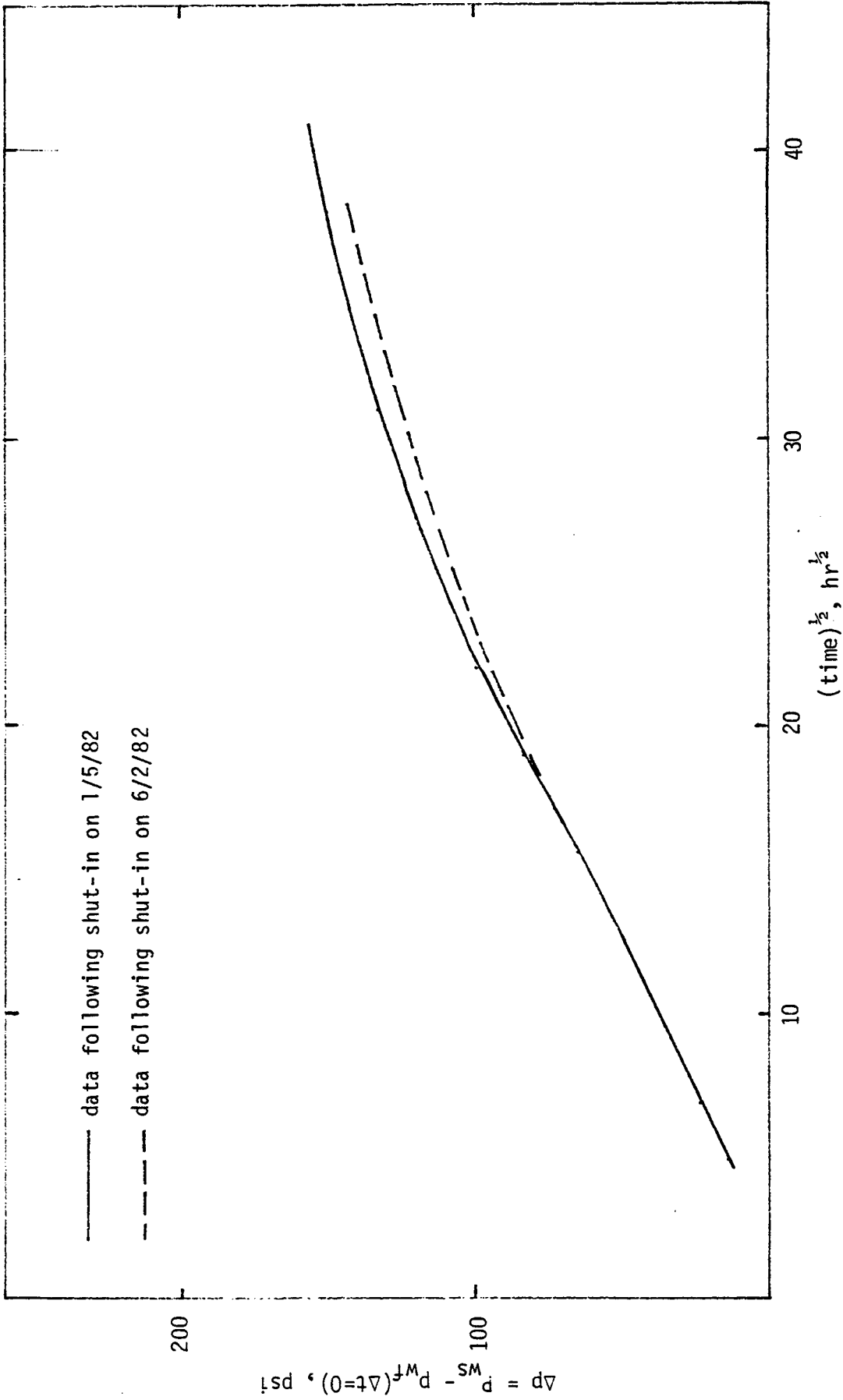


Figure 28. Square root data plot of pressure buildup for WIPP-12.

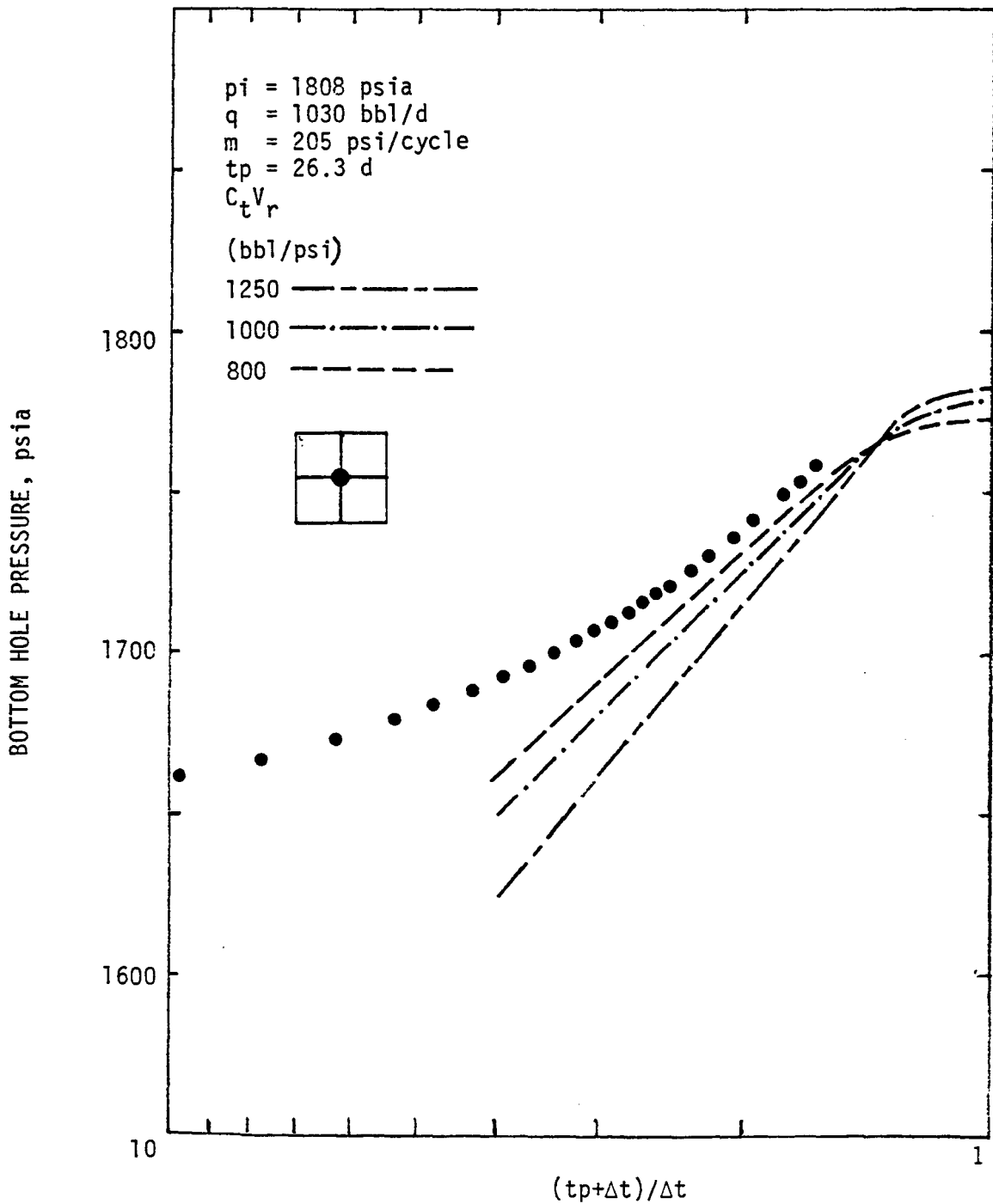


Figure 29. Horner plot of shut-in pressure for WIPP-12 following flow test #3. The circles are selected data points. The dashed lines are theoretically calculated pressure buildups for the parameters and geometry indicated in the upper left hand corner.

3.4 Flow Data

Figures 30 and 31 show the discharge rates versus time for the two flow tests conducted at the end of May, 1982. For flow test #2, the discharge rate decays exponentially with a half life of 0.43 days. For flow test #3, the picture is complicated by blockage of flow due to salt crystallizing within the pipes. However, the data does indicate a sum of two exponential (see dashed line on Figure 31). One exponential term decays with a half-life of about one day. The second exponential term cannot be estimated because of complications by blockage of flow due to salt crystallization. As mentioned in section 2.4 and as summarized in appendix A, the flow rate versus time for a two porosity system under constant drawdown testing is essentially a sum of two exponential terms. Flow test #3 thus indicates that the brine reservoir encountered at WIPP-12 is a two porosity system since it is believed that the test was of the constant drawdown type.

In appendix A it is shown that the product of compressibility and volume for the first porosity is given by

$$(c_t V_r)_f = 1.44 q(0) T_{1/2} / (p_i - p_{wf})$$

For flow test #2 we have the following parameters:

$$q(0) = 340 \text{ gpm} = 11,660 \text{ bbl/d}$$

$$T_{1/2} = 0.43 \text{ d.}$$

$$p_i - p_{wf} = 1808 - 1740 = 68 \text{ psi}$$

hence $(c_t V_r)_f = 106 \text{ bbl/psi}$. For flow test #3 we have the following parameters

$$q(0) = 400 \text{ gpm} = 13,710 \text{ bbl/d}$$

$$T_{1/2} = 1 \text{ d}$$

$$p_i - p_{wf} = 1808 - 1631 = 177 \text{ psi}$$

hence $(c_t V_r)_f = 112 \text{ bbl/psi}$. It will be shown in section 4.3 that $C_t V_r$ is about 1100 bbl/psi. Hence, the data indicate that the brine stored in the fracture volume is much less than the brine stored in the matrix volume.

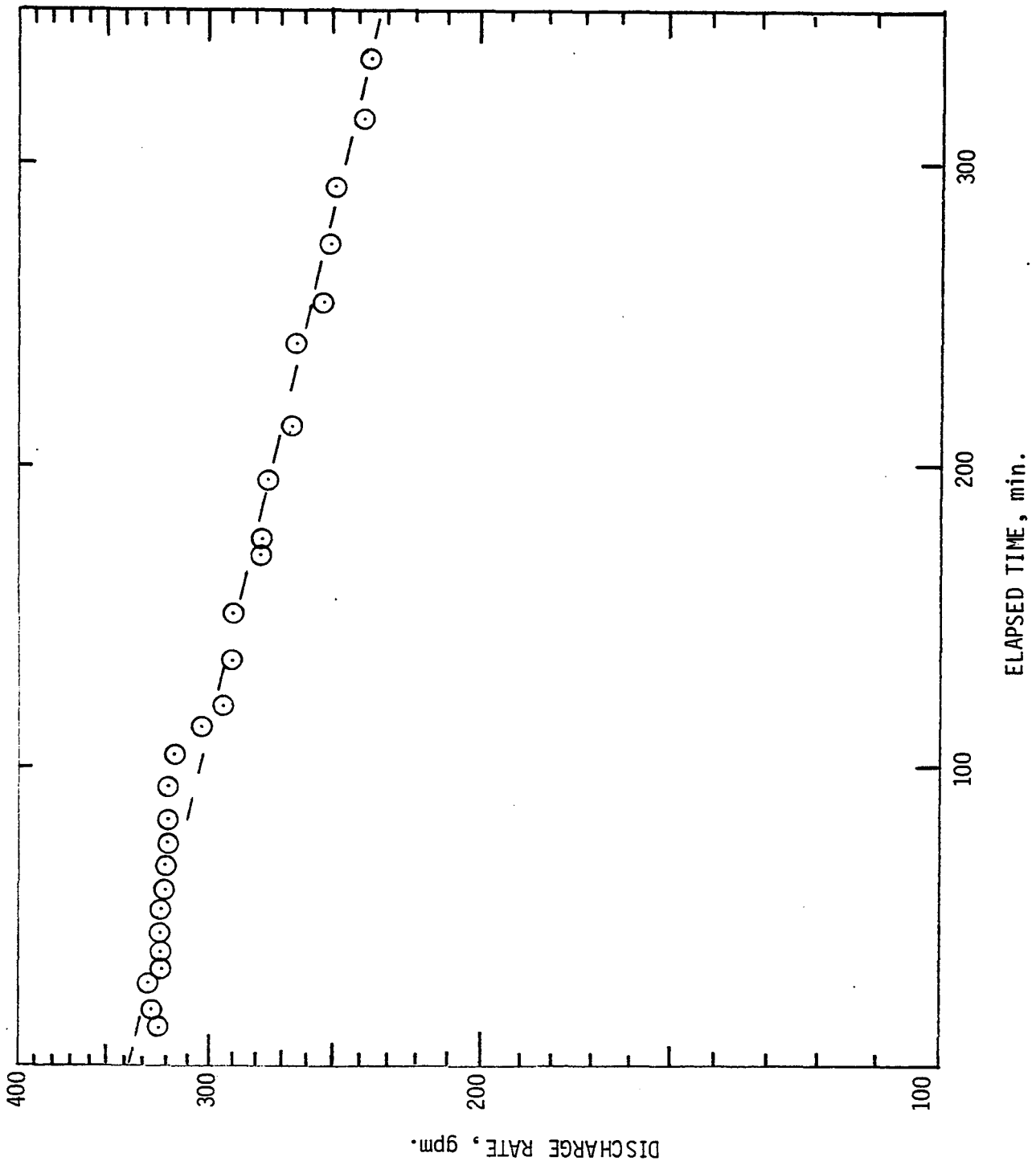


Figure 30. Semi-log plot of flow rate versus time for flow test #2 at WIPP-12.

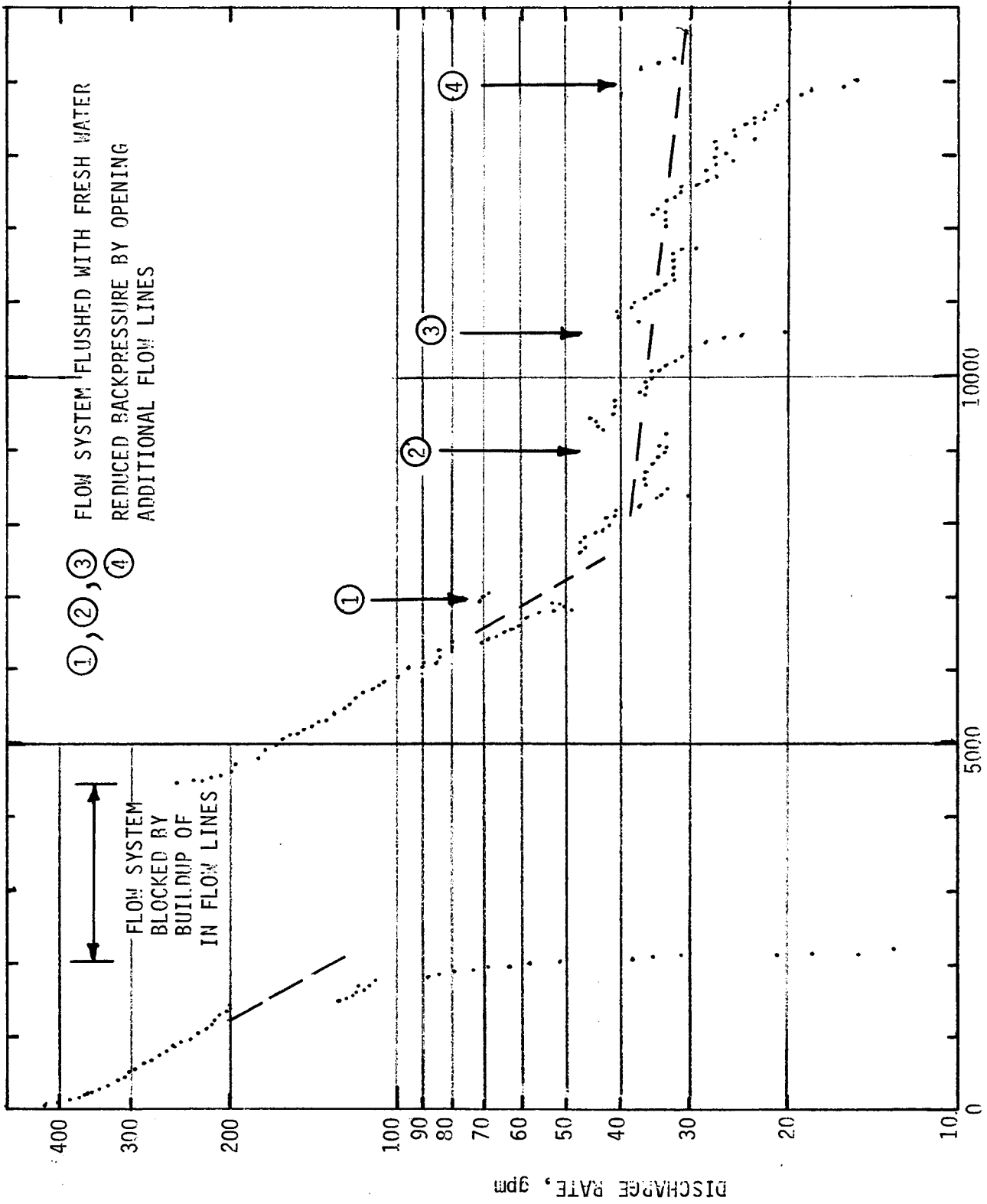


Figure 31. Semilog plot of flow rate versus time for flow test #3 at WIPP-12.

4 EXPLANATION OF THE BRINE RESERVOIRS NEAR THE WIPP SITE

4.1 Pore Volume Compressibility of Fractured Reservoirs

No data could be found in the petroleum literature on the pore volume compressibility of fractured reservoirs. The hydrologic literature suggests a compressibility range for jointed rock aquifers of 10^{-8} to 10^{-10} Pa^{-1} (7×10^{-5} to 7×10^{-7} psi^{-1}) (ref. 5). The pore volume compressibility can be estimated by dividing this range by the porosity. The compressibility of a reservoir can be measured by interference or pulse testing, a technique not useable at present since it requires a second well.

A number of theoretical papers on the influence of cracks and pores on the compressibility of rocks have been published in the geophysical literature since a pioneering paper by Eshelby (ref. 6). The purpose of many of these papers is to predict the velocity of seismic waves in fractured rock. In a paper by Walsh one can find the following expressions for penny shaped cracks (ref. 7).

$$\text{Volume of crack } V_C = \frac{4}{3} \pi a^3 \alpha \quad (5)$$

rate of change of porosity with pressure

$$\frac{d\phi}{dp} = - \frac{16}{9} c_r \frac{(1-\sigma^2)}{(1-2\sigma)} \frac{a^3}{V_C} \quad (6)$$

$$\frac{d\phi}{dp} = \frac{4}{3} \pi \frac{a^3}{3V_C} \frac{d\alpha}{dp} \quad (7)$$

pressure necessary to close a crack

$$p_C = \pi E \alpha / 4(1-\sigma^2) \quad (8)$$

Equation 8 is obtained by equating 6 and 7 and integrating the resulting equation. Further, by combining equations 5 and 7 one obtains the following expression for the pore volume compressibility.

$$c_f = \frac{1}{\phi} \frac{d\phi}{dp} = - \frac{4}{3\pi} \frac{(1-\sigma^2)}{(1-2\sigma)} \frac{c_r}{\alpha} = - \frac{4}{\pi} \frac{(1-\sigma^2)}{\alpha E} \quad (9)$$

since

$$c_r = 3(1-2\sigma)/E \quad (10)$$

The important conclusion in all these equations are that

$$p_c = \alpha E \quad (11)$$

$$c_f = \frac{1}{\alpha E} = \frac{1}{p_c} \quad (12)$$

For anhydrite we have the following values

$$E = 73 \text{ GPa} = 10.6 \times 10^6 \text{ psi}$$

$$\sigma = 0.3$$

$$c_f = 1.1 \times 10^{-7} / \alpha \quad \text{psi}^{-1}$$

$$p_c = 9.1 \times 10^6 \alpha \quad \text{psi}$$

or

$$c_f = 1.1 \times 10^{-7} / \alpha \quad \text{psi}^{-1}$$

$$p_c = 9.1 \times 10^6 \alpha \quad \text{psi}$$

The total reservoir compressibility is given by

$$c_t = c_{br}\phi + c_f = c_f \quad (13)$$

The large crack encountered at WIPP-12 must be viewed as a collection of small cracks as illustrated in Figure 32. Their size will vary and equations 11 and 12 should be replaced by an integral over the size distribution of the cracks. However, to keep the analysis simple this will not be done.

At WIPP-12, the geostatic pressure is about 3000 psia and the hydrostatic pressure was 1800 psia before flowing of the reservoir. Hence, the rock was under an effective pressure of 1200 psi. Cracks with an aspect ratio smaller than 1.3×10^{-4} cannot stay open and the highest pore volume compressibility is $830 \times 10^{-6} \text{ psi}^{-1}$ or 280 times that of water. At ERDA-6 similar calculations yield a smallest aspect ratio of 7.1×10^{-5} and a compressibility of 1540×10^6 or 510 times that of water.

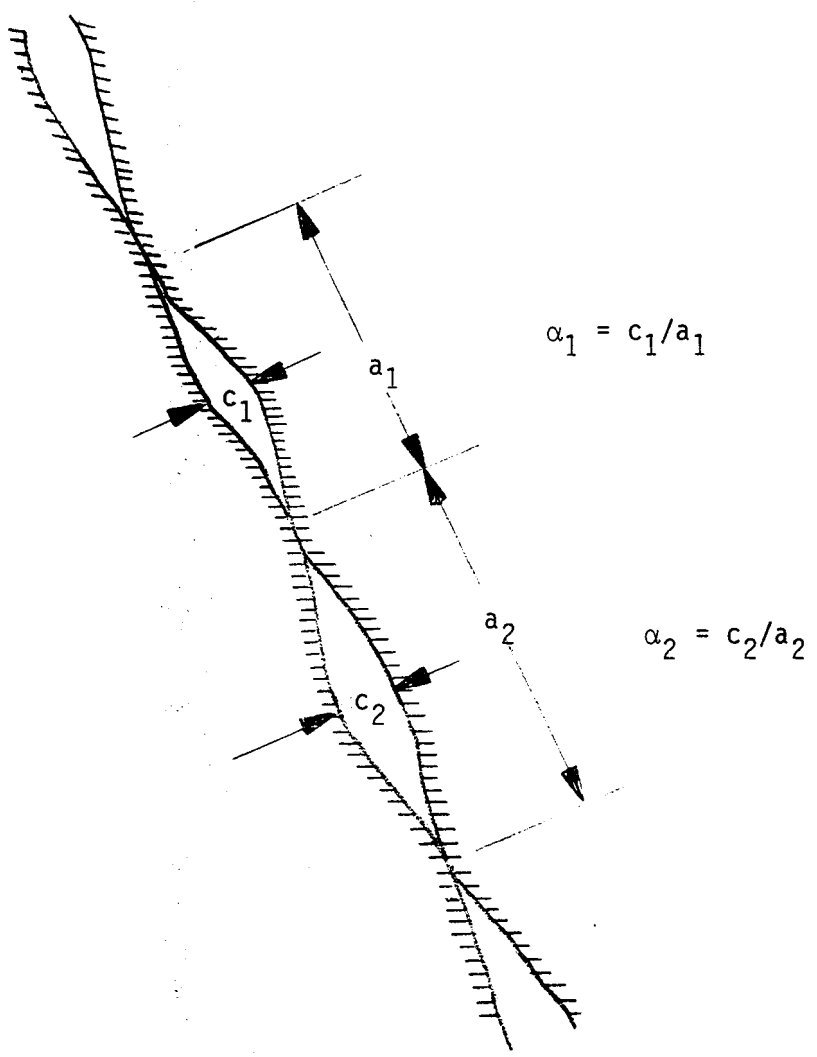


Figure 32. Breaking up of a large fracture into a series of small penny shaped cavities.

These theoretical considerations suggest that a total compressibility of about two orders of magnitude greater than the compressibility of water is not an unreasonable assumption and values of 125×10^{-6} to 250×10^{-6} psi^{-1} will be used in estimating the volumes of the reservoirs.

4.2 Estimated Volume of ERDA-6

The volume of the reservoir is estimated from a knowledge of the product of compressibility and volume, $c_t V_r$, which is obtained either from

- (1) stabilized pressures before and after flow and total outflow of brine
- (2) pressure buildup data
- (3) flow rate versus time data from constant drawdown test

For ERDA-6, the total outflow was 2196 bbl. (see Figure 4). The highest recorded pressure was 2030 psia (second pressure buildup of DST 2680-2) and the hydrostatic pressure at the height of the transducer was 1410 psia. The excess pressure was greater than 620 psi. Following the flow test, the well head pressure stabilized near 470 psig. The outflow of brine resulted in a pressure loss greater than 150 psi. The product of compressibility and volume is

$$c_t V_r \leq \frac{2196}{150} = 15 \text{ bbl/psi}$$

This value is in fair agreement with the values of 10 bbl/psi obtained from pressure buildup analysis. Figure 33 has a plot of reservoir volume versus compressibility for ERDA-6 assuming $c_t V_r$ is 15 bbl/psi. For compressibility values of 125×10^{-6} to 250×10^{-6} psi^{-1} , the volume is estimated to be 120,000 to 60,000 bb.

4.3 Estimated Volume of WIPP-12

Prior to shut-in on January 5, 1982, the total outflow of brine was 59,006 bbl (see Figure 21). The highest recorded pressure was 208 psig following an initial brine outflow of 3257 bbl. Following shut-in, the well head pressure

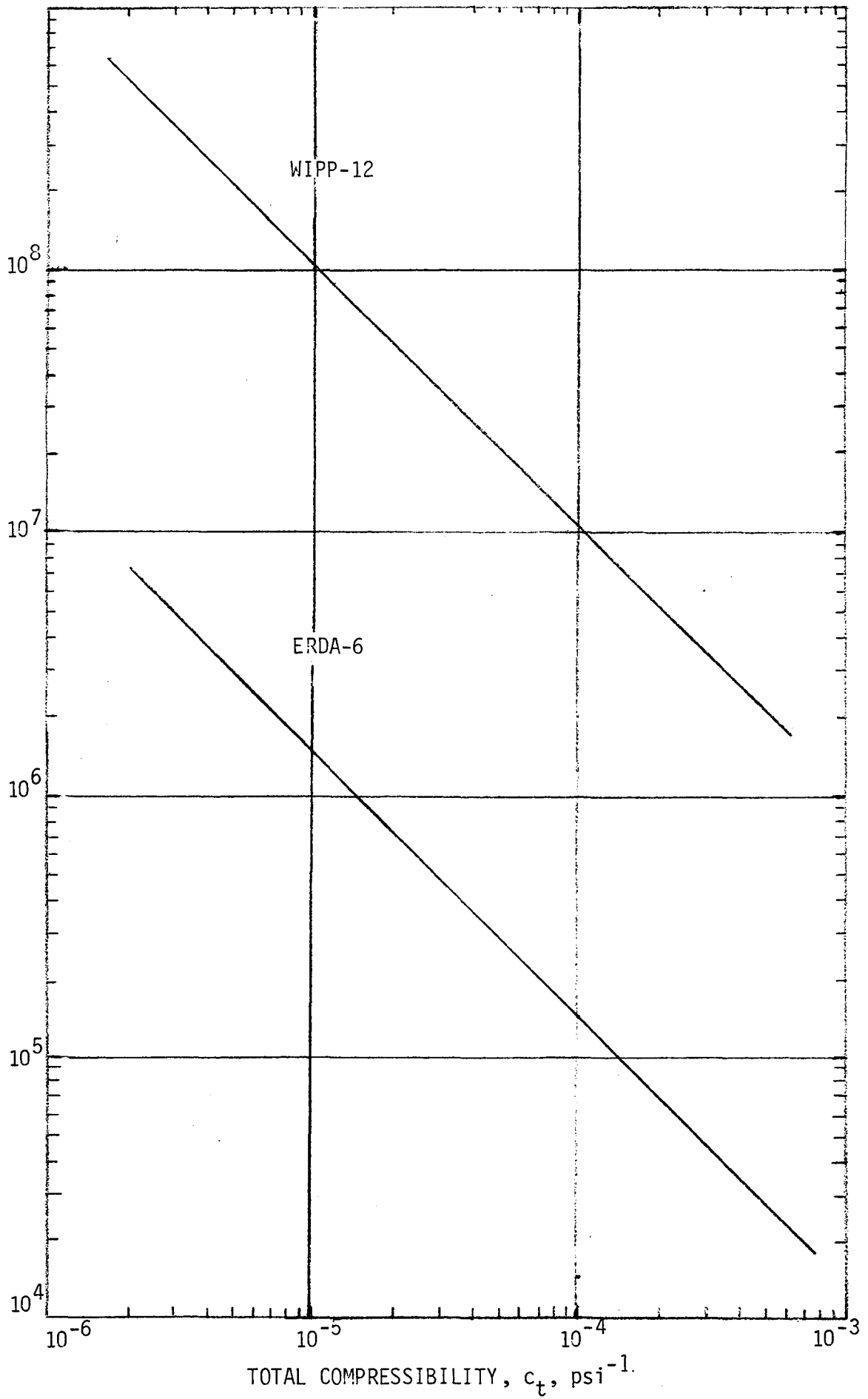


FIGURE 33. Volume of reservoir as a function of total compressibility,

built back up to 170 psig. The loss of excess pressure was at least 38 psi. The product of compressibility and volume is

$$c_t V_r \leq \frac{55749}{38} = 1470 \text{ bbl/psi}$$

For the flow test performed during the last week of May 1982, the total outflow of brine was 27,058 bbl. The loss of excess pressure appears to have been about 25 psi (the pressure buildup had not ceased at the time of the writing of this report). The product of compressibility and volume is about 1100 bbl/psi, which in good agreement with the value obtained from pressure buildup analysis. Figure 33 has a plot of reservoir volume versus compressibility for WIPP-12 assuming $c_t V_r$ is 1100 bbl/psi. For compressibility values of 125×10^{-6} to $250 \times 10^{-6} \text{ psi}^{-1}$, the volume is estimated to be 8.8×10^6 to 4.4×10^6 bbl.

4.4 Cause of Abnormal Pressure and Age of Reservoirs

An explanation of brine reservoirs in the Castile Formation must include a discussion of abnormal pressures and the formation of near vertical fractures in the anhydrite layers. In what follows, hypotheses that take into account the history of the basin will be presented. It is realized that these hypotheses are not the only explanations. However, it is expected that the discussion of these hypotheses will help resolve the brine reservoir issue.

The petroleum geologists have given special attention to the subject of abnormal formation pressures because they constitute an expensive and dangerous hazard in drilling. Bradley (ref. 8) has listed many factors including the following ones for the formation of abnormal pressures:

1. Epeirogenic movements such as the uplifting of the reservoir, or the equivalent, surface erosion, both of which result in the water pressure in the reservoir being too high for its depth of burial.
2. Thermal expansion or contraction of fluids reacting to temperature changes; an increase in temperature of one degree Fahrenheit can cause an increase of 125 psi in a sealed fresh water system.

3. Osmosis between waters having different salinity; sealing shale beds can act as semi-permeable membrane.
4. Chemical and/or biological action within pore waters trapped in a sealed formation.

These factors are interactive. For instance, if a reservoir is uplifted the resulting overpressure is partially alleviated by a decrease in reservoir temperature. However, the Delaware Basin has an unusually low Geothermal gradient of 0.3°F per 100 feet (ref. 9).

For petroleum reservoirs, Bradley believes that temperature increase with depth of burial is the most important factor for the formation of abnormal pressures. Many petroleum geologists disagree with him and attribute abnormal formation pressures to the compaction of sediments by the weight of overburden (refs. 10, 11). In some areas, the abnormal formation pressures have been attributed to tectonic activity (ref. 11). However, there is no indications of recent tectonic activity near the WIPP site.

The first explanation given by Bradley, uplift of reservoir as a result of surface erosion, is a plausible explanation for the Delaware Basin. Five million years ago, the WIPP site was covered with the Ogallala formation. Today it has completely eroded away (ref. 12).

Two explanations can be advanced for the formation of near vertical fractures in the anhydrite layers.

1. The fractures were caused by diapirism that created the anticlines. This explanation is illustrated in Figure 34.
2. The fractures were caused by the tilting of the Delaware Basin in the west. This tilting is illustrated in Figure 35.

The first explanation is supported by the assertion that most brine encounters have been associated with anticline structures. Anticlines have been observed at ERDA-6 and WIPP-12, but their occurrence at other brine encounters has not been definitively demonstrated. However, the strain (fractures

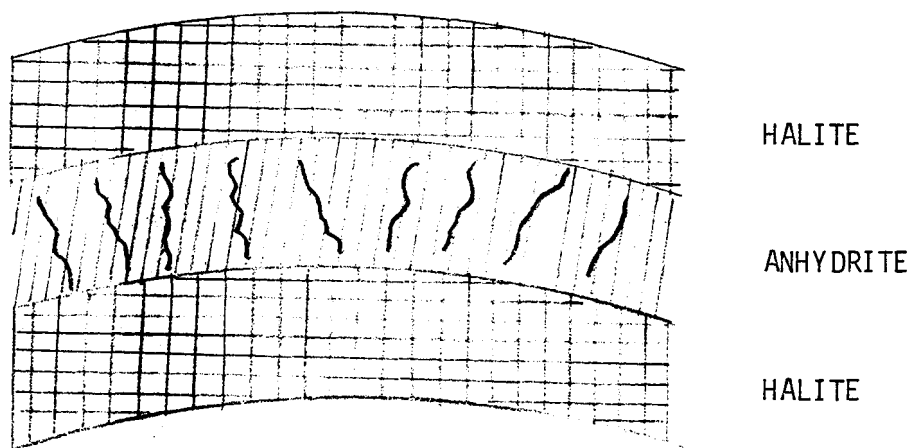
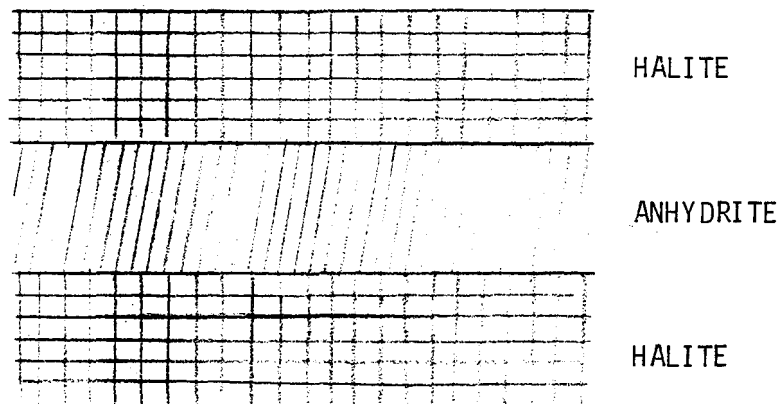


FIGURE 34. Formation of near vertical fractures in anhydrite from buckling of halite and anhydrite beds.

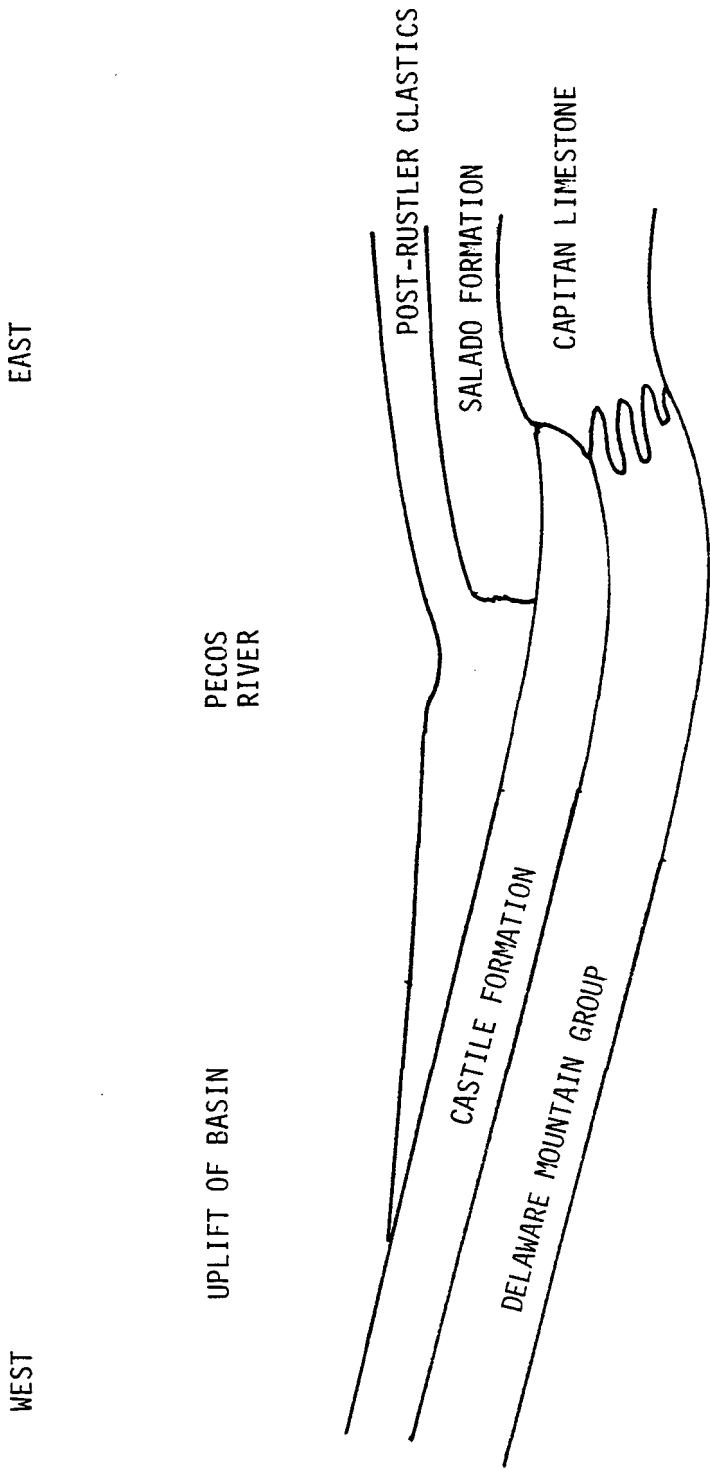


FIGURE 35. Diagrammatic cross section through the northern Delaware Basin, New Mexico. Figure based on Figure 3.3-2 of reference 13. Figure not to scale.

containing brine) should occur on the upper surface of the anhydrite layers. At ERDA-6 and WIPP-12, the fractures were encountered near the lower surface of the anhydrite layers.* This observation is in support of the second explanation.

As a result of the above considerations, the following explanation is suggested for the abnormal pressures of brine reservoir in the Castile formation.

- (1) The brine reservoirs in the Castile Formation were formed at the same time as the fracturing of the anhydrite layers.
- (2) Large amount of brine accumulated in areas of high fracture density (so called areas of structure).
- (3) The anhydrite layers were at greater depths than today; the fractures were connected to the surface, and the brine was at hydrostatic pressure. This assumption requires that the network of fractures propagated laterally to great distances. Certainly as far as the Capitan Limestone Formation. Vertical fractures through the Salado Formation are not plausible.
- (4) In time, many fractures sealed resulting in isolated reservoirs.
- (5) Because of erosion to the surface, the surface moved closer to the reservoirs. Because the reservoirs were sealed, they maintained the hydrostatic pressures of greater depths. This is illustrated in Figure 36.

*At Belco Hudson Federal, a borehole about 3 miles southwest of the center of WIPP site, the brine reservoir was also encountered near the lower surface of Anhydrite III, which is the same stratigraphy as for WIPP-12 (ref. 14). At Pogo, about 6 miles northeast of the center of the WIPP site, the brine was encountered in the middle of a 600 feet thick anhydrite layer that is a combination of anhydrite II and III. Halite II is missing at Pogo. At Union Federal, a borehole north of ERDA-6 and close to Pogo, the brine was also encountered at the lower surface of Anhydrite III. The Halite II is very thin but discernible. (The data for the last two borehole will be published in a forthcoming SANDIA document).

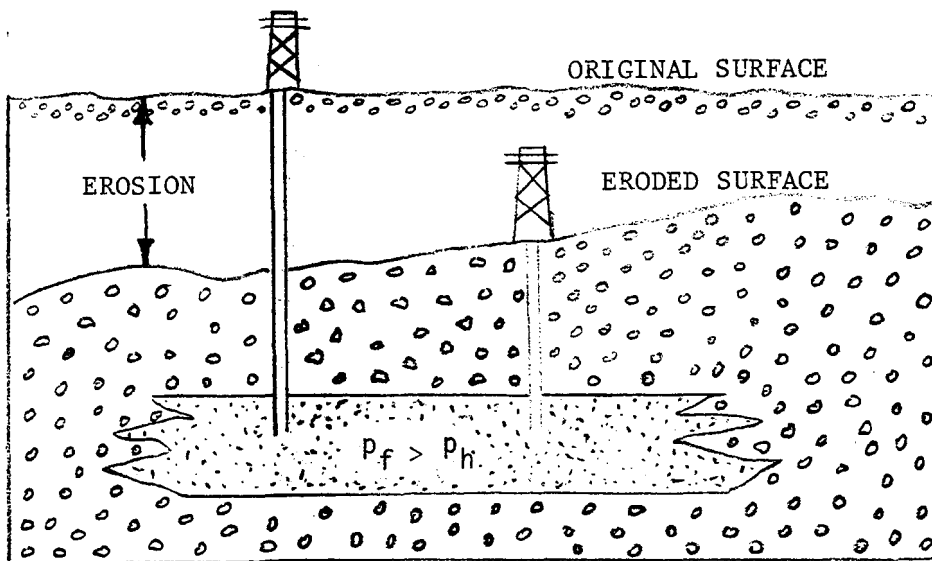


FIGURE 36. Formation of abnormal pressure as a result of erosion. p_f is the inherited formation pressure while p_h is the hydrostatic pressure. Figure taken from Reference 8.

(6) The excess pressure of a reservoir is a measure of the depth at which the reservoir was isolated from hydrostatic equilibrium. For ERDA-6, the excess pressure is about 600 psi. Since the hydrostatic gradient due to brine is 0.53 psi/ft, ERDA-6 was sealed from the surface when it was at a depth of

$$2710 + 600/0.53 = 3842 \text{ ft.}$$

For WIPP-12, the excess pressure is about 210 psi; WIPP-12 was sealed from the surface when it was at a depth of

$$3010 + 210/0.53 = 3406 \text{ ft.}$$

(7) The reservoirs must have begun forming when the anhydrite layers were at least 1000 feet lower from the surface than they are today (ref. 15). This must have been several million years ago, probably with the uplifting of the basin in the west.

A second explanation, a somewhat modified version of the previous explanation, is also based on the history of the basin (ref. 12). Bachman suggests that the hydraulic head of the Capitan aquifer system was higher during Gatuna time (600,000 + years ago). Following that time, the Pecos river entrenched itself in its present position and began scissoring into the Capitan aquifer system in the vicinity of Carlsbad. The interception lowered the hydraulic head by creating the Carlsbad Springs. These considerations suggest the following explanation:

1. The waters migrated from the Capitan Limestone Formation to the Castile Formation at the earliest stage of the formation of the Capitan aquifer.
2. The brines acquired a hydraulic head corresponding to the water level in the Capitan Limestone Formation at that time.
3. The brine reservoirs in the Castile Formation were isolated from the Capitan Limestone Formation as a result of sealing of fractures. Erosion reduced the ground level by about 1000 feet (ref. 15).

4. The pressure of the brine reservoirs is related to the water level that prevailed in the Capitan Limestone Formation millions of years ago.

To reconcile this explanation with the geochemistry of brines, it must be assumed that the early waters in the Capitan Limestone Formation were trapped seawaters. Independent analysis by EEG of the geochemical data will be published in subsequent reports.

4.5 Correlation of Hydrologic and Seismic Data

A large number of seismic profiles have been run over the WIPP site. SANDIA National Laboratory has used these profiles to construct a number of seismic structure maps. The top of the Castile formation map and the mid Castile Formation map are illustrated in Figures 37 and 38. The maps clearly show an anticlinal dome beneath the WIPP-12 borehole. Also shown is the extent of a 5 million barrel circular reservoir with a height of 150 feet and an equivalent porosity of 2%. The reservoir covers the extent of the anticlinal dome. If we are dealing with an anticlinal trap reservoir, then the seismic data support a reservoir size of 5 million barrels or less.

5. EFFECT OF WELL TESTING DATA ON DRILLING SCENARIO

It has been postulated that in future time when institutional control has been lost over the site, the void space in the waste storage area is flooded with brine as a result of an exploratory borehole connecting the repository and an underlying brine reservoir (ref. 16). A subsequent penetration of the repository by another borehole many years later results in contaminated brine flowing to the surface.

The hydrologic data obtained at WIPP-12 allows a more precise formulation of this scenario. The excess pressure of the reservoir with respect to the horizon of the repository is about 1375 psi (assume reservoir at a pressure of 1800 psia, hydrostatic gradient is 0.53 psi/ft, repository is 800 ft above brine reservoir). The amount of brine that could flow into the void of the waste storage area is

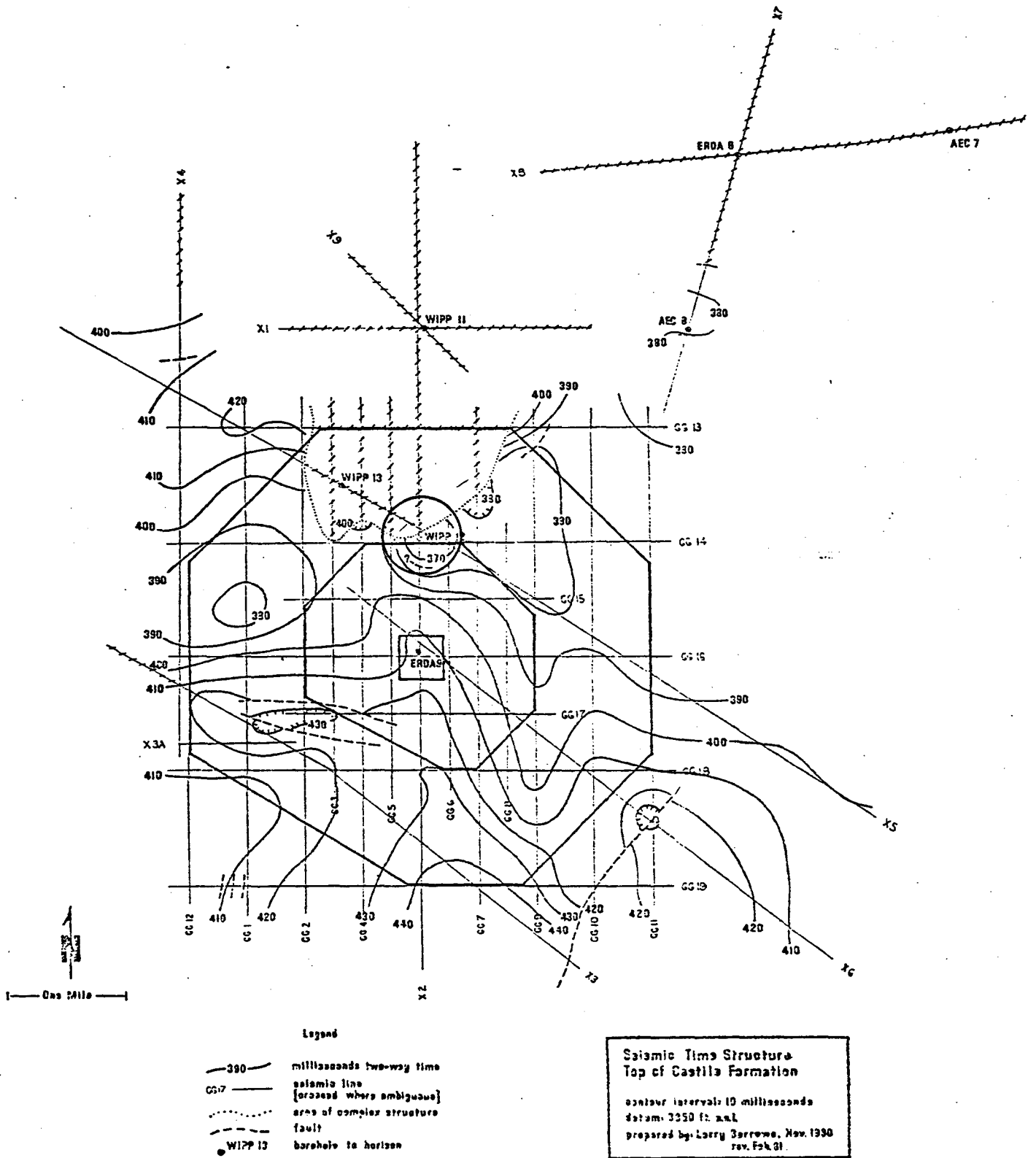


Figure 37. Extent (circle) of a 5×10^6 bbl reservoir with a height of 150 ft. and equivalent porosity of 0.02. Seismic data to be published in a forthcoming SNL report.

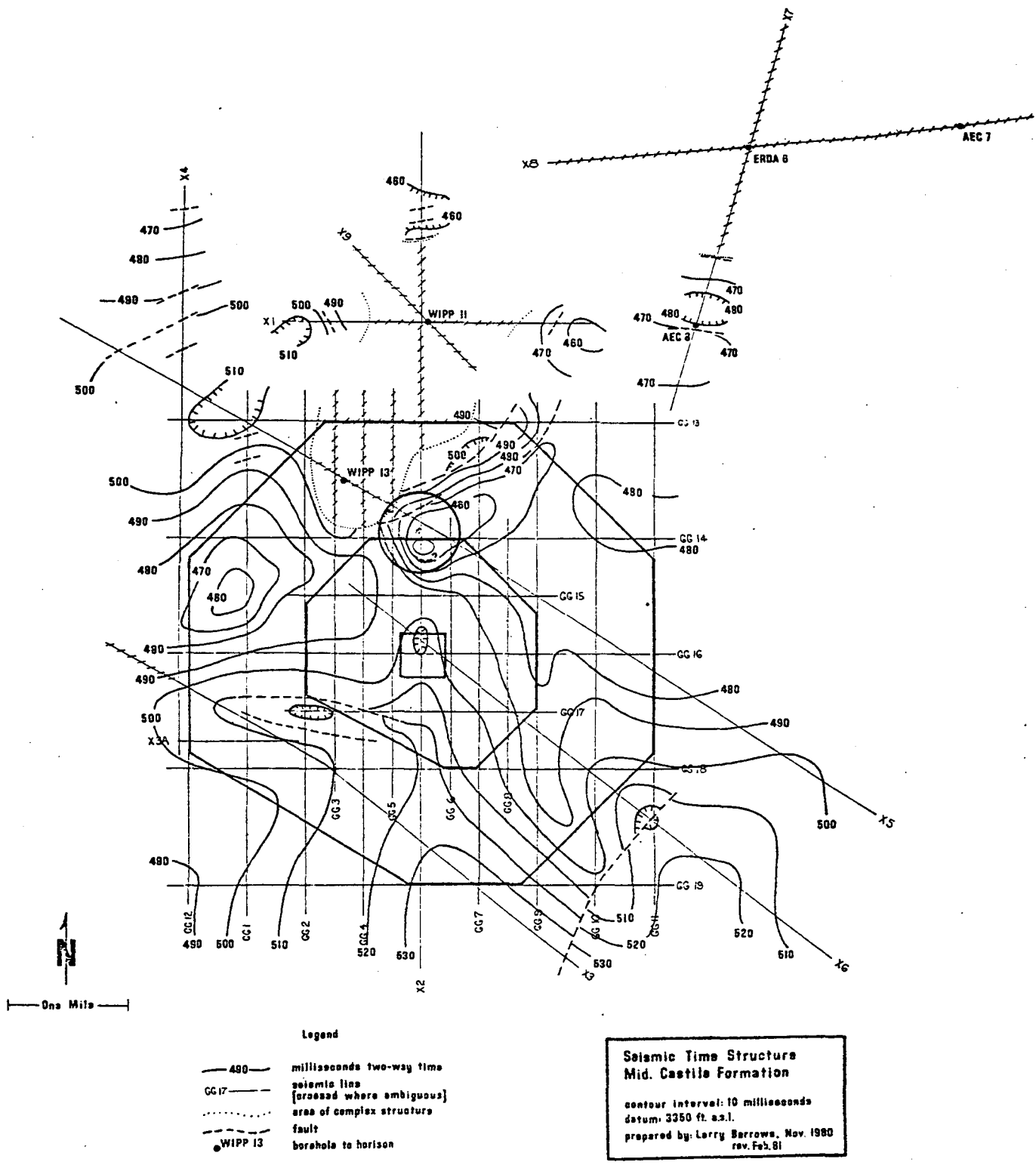


Figure 38 Extent (circle) of a 5×10^6 bbl reservoir with a height of 150 ft. and equivalent porosity of 0.02. Seismic data to be published in a forthcoming SNL report.

$$1100 \text{ bbl/psi} \times 1375 \text{ psi} = 1.51 \times 10^6 \text{ bbl}$$

However, if such a flow were to occur and if that much void space were available, then no flow to the surface would be possible because the brine would be at a negative pressure of 1140 psi with respect to the surface. In fact, since following shut-in on June 2, 1982, the WIPP-12 reservoir has indicated excess pressure of about 150 psi with respect to the surface. The maximum possible flow to the surface is

$$1100 \text{ bbl/psi} \times 150 = 165,000 \text{ bbl}$$

To be able to flow to the surface following a drilling scenario, the contaminated brine in the repository would have to be repressurized to 1140 psig. The creep of salt could pressurize the brine to lithostatic pressure, or about 2150 psig, after a long period of time. However, it must be assumed that the connection between the repository horizon and the reservoir is sealed otherwise the creep of salt would slowly force the brine back into the reservoir where it can reside at a pressure of about 1800 psia. This back flow would result in dilution of the radioactivity in the contaminated brine.

Hence it is very conservative to assume that the brine in the waste storage area becomes an isolated reservoir at lithostatic pressure. The compressibility of this reservoir must then be $2 \times 10^{-6} \text{ psi}^{-1}$, the compressibility of the brine. The excess pressure of the reservoir with respect to the surface will be 1040 psi. If this reservoir is now intercepted by another borehole, the maximum outflow of contaminated brine at the surface will be

$$1.51 \times 10^6 \text{ bbl} \times 2 \times 10^{-6} \text{ psi}^{-1} \times 1040 \text{ psi} = 3150 \text{ bbl.}$$

A more sophisticated version of the intrusion scenario would also include the formation of a gas bubble. Let us assume that the available void space is 1.5×10^6 bbl, and, as the brine flows into the repository following the first drillhole, all the air is compressed into a gas bubble. Eventually, because of the creep of salt, the bubble is pressurized to the lithostatic pressure and its volume is reduced to 9,700 bbl. It must now be assumed that the

second drillhole intercepts the brine only. As the gas depressurizes to the hydrostatic pressure, the volume of the bubble increases to 18,300 bbl and 8,600 bbl of brine are expelled at the surface. The total brine outflow could then reach 12,000 bbl (8,600 bbl + 3150 bbl). However, if the second drillhole intercepts the gas bubble directly, then no brine would flow to the surface.

APPENDIX A

Analytical tools for Characterizing Two-Porosity Systems

The basic partial differential equations for fluid flow in a two-porosity system were first presented by Warren and Roots (ref. 17) in 1963. In dimensionless form the equations contain the following four parameters.

Dimensionless radius

$$r_D = r/r_w \quad \text{A-1}$$

Dimensionless time

$$t_D = \frac{2.637 \times 10^{-4} k_f t}{[(\phi c_t)_f + (\phi c)_{ma}] \mu r_w^2} \quad \text{A-2}$$

Dimensionless fracture storage parameter

$$F_{ft} = \frac{(\phi c)_f}{(\phi c)_f + (\phi c)_{ma}} \quad \text{A-3}$$

Dimensionless matrix to fracture permeability ratio

$$\epsilon = \alpha_{ip} \frac{k_{ma}}{k_f} r_w^2 \quad \text{A-4}$$

Warren and Roots as well as Kazemi (ref. 18) showed how to analyze two-porosity data when the straight lines are parallel as illustrated in Figure 39. The parameter F_{ft} is estimated from δp while ϵ is obtained from theoretical considerations. Uldrich and Ershaghi (ref. 19) showed how to estimate both F_{ft} and ϵ from a knowledge of Δt^* , p_{ws}^* and $(p_{ws}^*)_{\text{early}}$ or $(p_{ws}^*)_{\text{late}}$ (see Figure 39 for these quantities).

No method has yet been advanced for analyzing pressure buildup data when the straight lines are not parallel. No attempt was therefore made to apply the techniques to the ERDA-6 data.

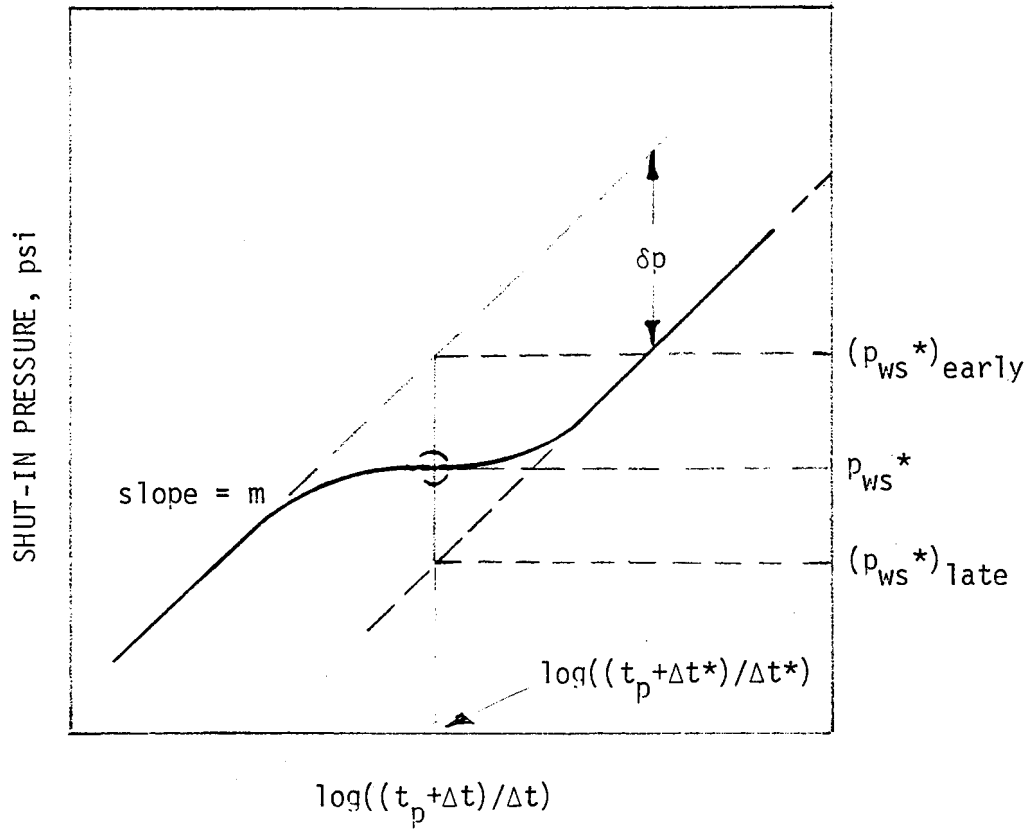


FIGURE 39. Schematic of pressure buildup for a two-porosity system.

For constant drawdown tests, techniques for analyzing the data have only been published recently (ref. 4). As indicated, the solutions behave as illustrated in Figure 16. The rigorous solution can be approximated by the sum of the long time solution for a noncommunicating matrix

$$q_D = \frac{1}{(\ln r_e - 3/4)} \exp\left[\frac{-2}{r_e^2 (\ln r_e - 3/4)} \frac{t_D}{F_{ft}}\right] \quad A-5$$

and the long time solution

$$q_D = \left[\frac{r_e^2 - 1}{2}\right] F_{ft} \exp\left(-\frac{\epsilon}{1 - F_{ft}} t_D\right) \quad A-6$$

From equation A-5, we obtain for the product of fracture volume times fracture compressibility

$$(\phi c_t)_f \pi r_e^2 h = (c_t V_r)_f = \frac{1.44 T_{1/2} q(o)}{(p_i - p_{wf})} \quad A-7$$

NOMENCLATURE

- a = Half-length of major axis of penny shaped crack
- C_A = Shape constant or factor
- c_{br} = brine compressibility, psi^{-1}
- c_f = pore volume compressibility, psi^{-1}
- c_r = compressibility of rock, psi^{-1}
- c_t = system total compressibility, psi^{-1}
- E = Young's Modulus of reservoir rock, psi
- F_{ft} = ratio of porosity-compressibility product of fracture to total porosity compressibility product of reservoir
- h = formation thickness, ft
- k = permeability, md
- k_f = fracture permeability, md
- k_{ma} = matrix permeability, md
- m = slope of linear portion of semilog plot of pressure transient data, psi/cycle
- ΔP_{ws} = pressure deviation from the linear buildup trend of the Horner plot
- p = pressure, psi
- p_c = pressure necessary to close penny shape crack, psi
- p_i = initial pressure, psi
- p_{wf} = flowing bottom-hole pressure, psi
- P_{DMBH} = Matthews-Brons-Hazebrook-type dimensionless pressure
- q = flow rate before shut-in bbl/d
- q_D = dimensionless flow rate
- r_D = dimensionless radius
- r_e = effective radius of reservoir, ft
- r_{eD} = dimensionless outer boundary radius, r_e/r_w
- r_w = wellbore radius, ft
- t = time
- t_D = dimensionless time, see equations A-2
- t_{DA} = dimensionless producing time based on drainage area
- t_p = equivalent time well was on production before shut-in, days
- $T_{1/2}$ = half-life for flow rate time for flow rate to decrease to one half of its initial value.

v = Volume of region containing crack
 Δt = shut-in time, days
 Dt_{DA} = dimensionless shut-in time based on drainage area
 V_C = Volume of penny shaped crack
 V_r = Volume of reservoir, bbl
 α = aspect ratio of penny shaped crack, fraction
 α_{ip} = interporosity flow shape factor, fr-2
 ϵ = interporosity flow parameter
 μ = viscosity, cp
 ϕ = porosity, fraction
 $(\phi c)_f$ = porosity compressibility product of fractures
 $(\phi c)_{ma}$ = porosity compressibility product of matrix
 σ = Poisson's ratio, fraction

REFERENCES

1. D'Appolonia Consulting Engineers, Inc. Data File Report. ERDA-6 and WIPP-12 Testing. Waste Isolation Pilot Plant, Westinghouse Electric Corp. Project No. NM 78-648-811A/812B, 6 vols., February 1982.
2. Earlougher, R.C., Jr. Advances in Well Test Analysis. Society of Petroleum Engineers of Monograph of the Henry L. Doherty Series, 5. Dallas: AIMW, 1977.
3. Dake, L.P. Fundamentals of Reservoir Engineering. New York: Elsevier Scientific Publishing Co., 1978, p 213.
4. DaPrat, G., H. Cinco-Ley, and H.J. Ramey, Jr. Decline Curve Analysis Using Type Curves for Two-Porosity Systems, Soc. Pet. Eng. J., 354-362, June 1981.
5. Freeze, R. A., and J. A. Cherry. Groundwater. New Jersey: Prentice-Hall Inc., 1979.
6. Eshelby, J.D. The Determination of the Elastic Field of an Ellipsoidal Inclusion and Related Problems, Proc. Roy. Soc. London, A, 241, 376-396, 1957.
7. Walsh, J.B., The Effect of Cracks on the Compressibility of Rocks, J. Geophys. Res., 70 (2), 381-388, 1965.
8. Bradley, J.S., Abnormal Formation Pressure, AAPG Bull., 59, 957-973, 1975.
9. Dresser Atlas, Log Interpretation Fundamentals, Houston, TX, 1975.
10. Dickey, P.A., Abnormal Formation Pressure: Discussion, AAPG Bull., 60 1124-1128, 1976.

11. Chapman, R.E., Petroleum Geology, a Concise Study, New York: Elsevier Scientific Publishing Co., 1973, pp 67-76.
12. Bachman, G. O., Regional Geology and Cenozoic History of Pecos Region, Southeastern New Mexico, USGS Open-File Report 80-1099, 1980, pp 71-72.
13. Powers, D. W., Lambert, S. J., Shaffer, S. E., Hill, L. R., and Weart, W. D., Geologic Characterization Report, WIPP Site, Southeastern New Mexico, SAND 78-1596, Vol. 1, 1978.
14. Griswold, G. B. "Site Selection and Evaluation Studies of the Waste Isolation Pilot Plant (WIPP), Los Medanos, Eddy County, NM (SAND 77-0946)", 1977.
15. Anderson, R. Y., and Powers, D. W., Salt Anticlines in Castile-Salado Evaporite Sequence, Northern Delaware Basin, New Mexico, New Mexico Bureau of Mines and Mineral Resources Circular 159, May 1978.
16. Channell, J.K. "Calculated Radiation Doses from Radionuclides Brought to the Surface if Future Drilling Intercepts the WIPP Repository and Pressurized Brine", Report EEG-11, January 1982.
17. Warren, J.E., and P.J. Root, The Behavior of Naturally Fractured Reservoir, Soc. Pet. Eng. J., 245-255, Sept. 1963.
18. Kazemi, H., Pressure Transient Analysis of Natural Fractured Reservoirs with Uniform Fracture Distribution, Soc. Pet. Eng. J., 451-462, Dec. 1969.
19. Uldrich, D.O., and Iraj Ershaghi, A Method for Estimating the Interporosity Flow Parameter In Naturally Fractured Reservoirs, Soc. Pet. Eng. J., 324-332, Oct. 1979.